A THEORETICAL STUDY OF POWER RECIEVED IN TROPOSCATTER COMMUNICATION LINKS BASED ON LAYERED—ATMOSPHERE MODEL

A Thesis Submitted
In Partial Fulfilment of the Requirements
for the Degree of
MASTER OF TECHNOLOGY

by

Maj. M. S. VIRK

to the

DEPARTMENT OF ELECTRICAL ENGINEERING
INDIAN INSTITUTE OF TECHNOLOGY KANPUR
AUGUST 1977

CERTIFICATE

This is to certify that the thesis entitled 'A Theoretical Study of Power Received in Troposcatter Communication Links Based on Layered-Atmosphere Model', is a record of work carried out by Maj. M.S. Virk under my supervision and that it has not been submitted elsewhere for a degree.

N C Mathur

(N.C. MATHUR)
Professor
Department of Electrical Engineering
Indian Institute of Technology
KANPUR

August ,1977

ACKNOWLEDGEMENT

I sincerely thank Dr. N.C. Mathur for his valuable guidance , suggestions and help given for successful completion of this work.

Special thanks are due to Sqn.Ldr. P.R. Pande who spent a lot of his valuable time in assisting me debugging the computer program.

I also thank Shri J.S. Rawat for neat and efficient typing work.

KANPUR
AUGUST ,1977

Major M.S. VIRK

ABSTRACT

A forward scatter technique can be effectively used to probe troposphere for various parameters such as cross path wind velocity, isotropy/anisotropy of turbulence, layer heights, wave number dependence, exponent 'p' of turbulence spectrum and structure function C_n^2 with moderate variations. This can be achieved over extended common volume in space.

This thesis is the theoretical study of power received in troposcatter communication links based on layered-atmosphere model. The common volume is systematically moved through space by swinging receiver and transmitter antenna beams along as well as across the great circle path.

For this study, the atmosphere is assumed to possess layered-structure. The tropospheric conditions are simulated by considering various models of single turbulent layers of different vertical widths at different heights, multiple layers, with different suggested values of exponent 'p' and system response

obtained. Accurate scatter signals are evaluated by detailed estimation of common volume duly considering complex forward scatter geometry along the great circle path and at a horizontal distance from it. Although specular reflection does exist and is superimposed on the scatter signals, it has not been included in the simulated model.

TABLE OF CONTENTS

LIST OF ILLUSTRATIONS

CHAPTER I

INTRODUCTION

1.1 Historical Background:

From the first ever recorded troposcatter communication during 1932-33 by Marconi over a distance of 168 miles using 550 MHz, to the numerous present day models, attempts have been afoot to explain precisely all the observed facts in a troposcatter system.

The earlier models put forward to explain the propagation of short radio waves beyond radio horizon were based on

(a) Diffraction arround smooth earth
(b) Reflection from elevated layers caused by abrupt changes in the temperature and humidity of the earth's atmosphere and
(c) Duct propagation

All these models were not sufficient to satisfactorily explain propagation of radio waves between 50 MHz to 5 GHz over distances upto 1000 Kms. This led to the belief of some sort of scatter mechanism. This was further confirmed by the presence of fields at all times, though subject to rapid and severe fading.

The first theory of scatter mechanism was based on the theory of scattering from irregularities of dielectric

constant of troposphere caused by turbulence (Booker and Gordon, 1949) . Later, Villars and Weiskoff (1955) put forward different physical causes for refractive index fluctuations. Obukhoff's statistical theory of turbulence was applied to explain the problems of radio wave scattering (Silverman, 1956).

Although no single theory exists which explains all the observed facts of a troposcatter system, Tatarski's theory of wave propagation through turbulent medium (Tatarski, 1961) provides by far the most plausible explanation.

1.2 Atmospheric Microstructure:

The propagation of very high frequencies through lower atmosphere is controlled by the variations of the refractive index 'n'. The refractive index is in turn a function of temperature, pressure and humidity.

For frequencies less than 100 GHz, the value of refractivity N $(=(n-1)\times 10^6)$ is given by

$$N = 77.6 \frac{P}{T} + 375000 \frac{e}{T^2} \qquad (1.1)$$

correct upto 0.5% for

Pressure P between 200 and 1100 mb
Temperature T between 240° and 310°K
Partial pressure of water vapour less than 30 mb.

It has recently been shown by the use of high resolution microwave and accoustic radars, that there exists a wide variety of turbulent eddies having thicknesses ranging from 1 m to a few tens of meters. Large amplitude Kelvin-Helmholtz (K-H) waves have also been reported in the middle and upper troposphere. These are attributed to the dynamic instability of sheared stratified flow when Richardson number (Ri) $\leq 1/4$ (Birkemeiyer, 1974). The forward scatter reflectivity is dependent on the scale of eddies given by

$$L_f = \frac{\lambda}{2} \sin \theta/2 \qquad (1.2)$$

where λ is system wave length and θ is the scattering angle.

'L_f' may be called as "System-filtering scale". At normal frequencies of operation (upto a few GHz) the system is dependent on large scale turbulence structures. The micro scale turbulence which is also present in the layers, does not contribute significantly to the received signal.

But for shorter wave length, the scatter would be due to the smaller scale eddies. These occur more at higher altitudes. The fading, in such a case would be faster since the scatterers at higher altitudes are subjected to higher wind velocities. This also produces greater Doppler shifts.

Exact knowledge of refractivity obtained from in-situ measurements is essential for obtaining tropospheric microstructure for correct prediction. Unfortunately the microwave refractrometers, for this purpose, are not available in our country. However for 2.1 GHz KANPUR-NAINITAL link, set up by I.I.T. KANPUR, some in-situ measurements have been carried out (Mathur, Mehra and Raman, 1974) by flying the refractrometer over the propagation path. These measurements have revealed that the average value of scale of turbulence is of tens of meters and mean squared refractivity fluctuations ($\overline{\Delta n^2}$) about 10^{-11} for heights upto about 2300 meters.

1.3 Problem Defining:

A troposcatter link at 2.1 GHz has been established between KANPUR and NAINITAL (a distance of 330 Kms) and a lot of data has been logged over this link. Initial simulation for this link was developed by using the concept of atmospheric structures consisting of layered scatterers (Gupta, 1973). Later a study of troposcatter signal characteristics, based on the random layered scatter model, assuming that the power received is proportional to (-11/3)th power of the scattering angle 'θ' was carried out.(Bassi, 1974).

Several troposcatter parameters such as cross path wind velocity, scattering layer height, isotropy/ anisotropy of turbulence, wave number dependence, exponent (p) of the spectrum of turbulence, including specular reflection contribution to the signal level can be determined by means of scatter experiments involving measurement of spectrum of received signal, average doppler shift and total power received as a function of the antenna beam off-set.

For Kanpur-Nainital link, for various assumed values of the above referred parameters, doppler cross wind relations have already been calculated and plotted (Mathur and Mehra, 1976).

A very large number of troposcatter experiments can be used as remote probing tools for tropospheric parameters (Gjessing, 1969). These fall within 7 main categories.

1) Experiments in beam swinging in horizontal and vertical planes.
2) Comparison of time-average power on several radio frequencies.
3) Measurements of vertical correlation distance of a field strength.
4) Measurement of horizontal correlation distance of the field strength.

5) Measurement of antenna to medium coupling loss.

6) Time-delay experiments (Rake-techniques).

7) Band width measurements (Frequency sweep experiments).

Beam swinging experiments can also be effectively used to determine the moderate variations of structure function C_n^2 (Gjessing, 1962).

In the case of various studies conducted for Kanpur-Nainital link, the received power (P_R) has been estimated based on NBS 101 report. According to this method, the value of the path loss is given as

$$L_{mp} = 30 \log f_{MHz} - 20 \log d + F(\theta d) + Aa \qquad (1.3)$$

where Aa = absorption loss and

F(θd) = Scatter loss, 'θ' being in radians and 'd' in Kms.

The scatter loss is given by the relation

$$F(\theta d) = K(N_s) + 0.34\ \theta d + 30 \log (\theta d)$$

where N_s is the surface refractivity and

$$K(N_s) = 139.5 + 0.06\ N_s - 2.4 \times 10^{-6}\ N_s^2 \qquad (1.4)$$

Thus the scatter loss as per NBS method is basically a function of scatter angle 'θ' and separation

between the transmitter and receiver. It is thus based on rough approximations. Further approximations used for calculation of the common volume in order to determine the received power leave a lot of room for improvement.

Attempts have thus been made, in this thesis to evaluate the total power received on Kanpur-Nainital link calculated on the basis of the layered atmosphere model with detailed analysis for more exact calculation of common volume. The factors which influence greatly the power received, the influence of which have been considered for received power calculations are

1) Height and thickness of the scattering layer.
2) Presence of more than one scattering layer within the common volume.
3) Beam swinging in different directions (influence of antenna pointing).
4) Sensitivity of the received power to the power index 'p' of refractivity turbulence spectrum. This is achieved by considering the average value as $p = 11/3$ with extreme values as $p=2$ and 5.

1.4 Break up of the work:

This work has been divided into various chapters. In chapter II, forward scatter geometry and various coordinate systems suitable for various types of scanning techniques are given in brief. Common volume environments with ray path considerations, geometry of the common volume and its evaluation based on Lanmer's method are discussed in chapter III. In chapter IV a brief description of scatter theory along with scatter-power evaluation and evaluation of scatter-integral are discussed. The effects of specular-reflection on the received signal level are included in chapter V. In the last chapter, discussions, conclusions and recommendations on future development if any are included.

CHAPTER II

FORWARD SCATTER GEOMETRY AND COORDINATE SYSTEMS

2.1 Forward scatter geometry:

The basic forward-scatter geometry indicating great circle plane geometry of the troposcatter path is given in Fig. 2.1.

In Fig. 2.1, R_X and T_X are the receiver and transmitter locations respectively. P is the scatter point which is assumed to be the center of the common volume. The centre is defined as the inter-section point of the antenna boresights. Elevation angle are α_{VR} and α_{VT} with α_{HR} and α_{HT} indicating the azimuthal angles. θ is the scattering angle which is defined as the angle between the transmitted signal ray and scattered signal ray towards the receiver at point P.

The extent of scattering is determined by the magnitude of fluctuationsof tropospheric refractivity at the scattering point ($\overline{\Delta N^2}$). The forward scattered power P_R is given as (Atlas etal, 1968).

$$P_R = \frac{P_T \lambda^2}{(4\pi)^3} \int_V \frac{G_R G_T \sigma(\theta)}{L_R^2 L_T^2} \, dV \qquad (2.1)$$

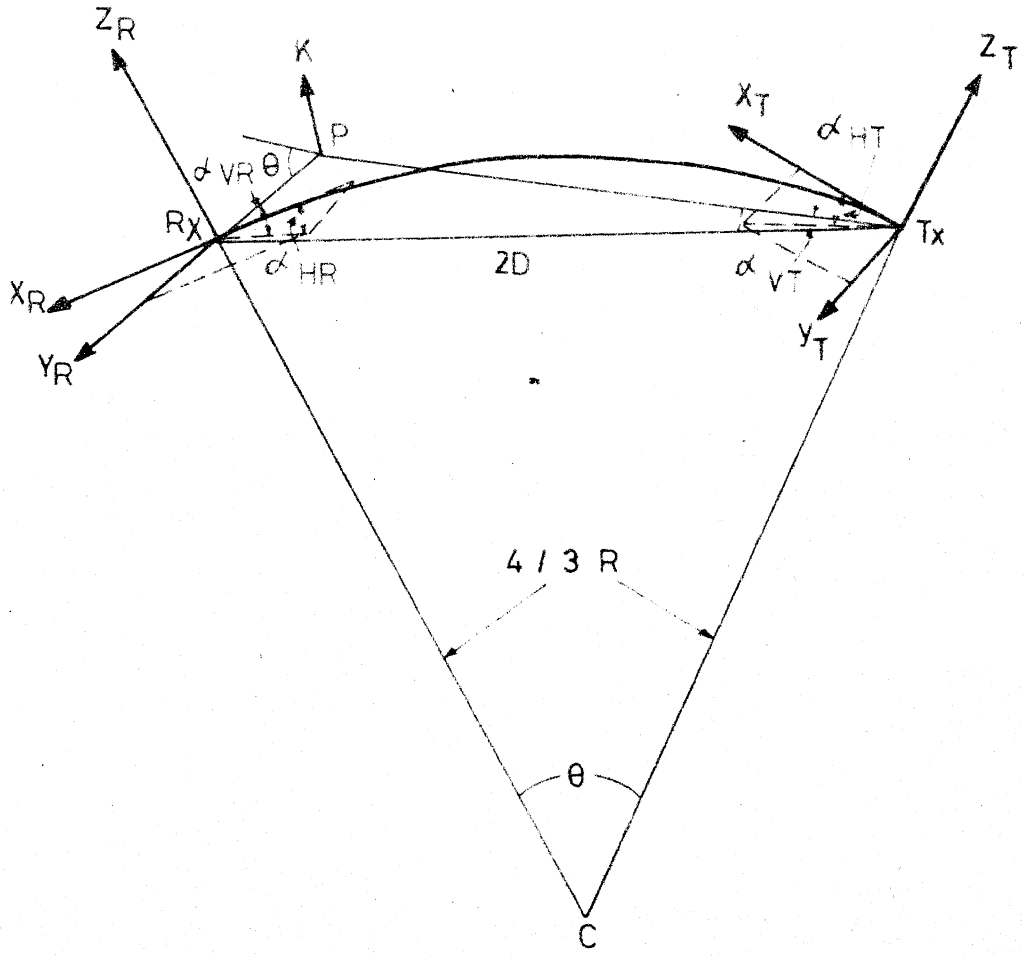

FIG. 2.1 BASIC SCATTER GEOMETRY

It is thus seen that the received power depends on

(a) Transmitted power P_T. More transmitted power, more would be the received power. But there are physical limitations deciding optimum value of P_T.

(b) The transmitter and receiver antenna gain functions G_T, G_R. The gain functions are dependent on the size and shape of the antennas and also on the system wavelength. However antenna size cannot be increased too much since it results in aperture-to-medium coupling loss.

(c) The distance of scatter point from the transmitter (L_T) and receiver (L_R). At larger values of L_T, L_R, the scattered power received will be appreciably reduced.

(d) Scattering angle 'θ' and power index 'p'. Even small increase in the value of θ reduces P_R considerable the values of the power index 'p' is generally accepted to be (11/3) (Tatarski, 1961; Gjessing, 1962). However, the extreme values of 2 and 5 are also considered.

(e) Scattering cross section $\sigma(\theta)$. It is defined as the power density of the scattered wave in the direction of receiver, per unit solid angle, per unit scatter volume per unit power density of the incident wave on the scatter volume.

(f) Common volume. It is in turn dependent on θ and antenna boresight inclination with the horizontal and the antenna beam width.

Power received is related through $\sigma(\theta)$ to the three dimensional power spectrum of the refractive index field $\phi_n(\bar{K})$ by the relation

$$\sigma(\theta) = \frac{\pi K^4}{2} \phi_n(\bar{K}) \qquad (2.2)$$

Considering Kolmogorov's theory of locally homogeneous turbulence and Obukhov's theory of passive admixture in the turbulent flow, the value of ϕ_n is given as

$$\phi_n(\bar{K}) = 0.033\, C_n^2\, K^{-11/3} = .033\, C_n^2\, (2k \sin\theta/2)^{-11/3} \qquad (2.3)$$

$\bar{K}$ is called the scattering vector. It is defined as the vector bisecting the angle made by the transmitter T_x, receiver R_x and the scatter point P. Geometry showing scattering vector is given in Fig. 2.2.

The magnitude of the scattering vector is given as

$$|\bar{K}| = \frac{4\pi}{\lambda} \sin(\theta/2) \qquad (2.4)$$

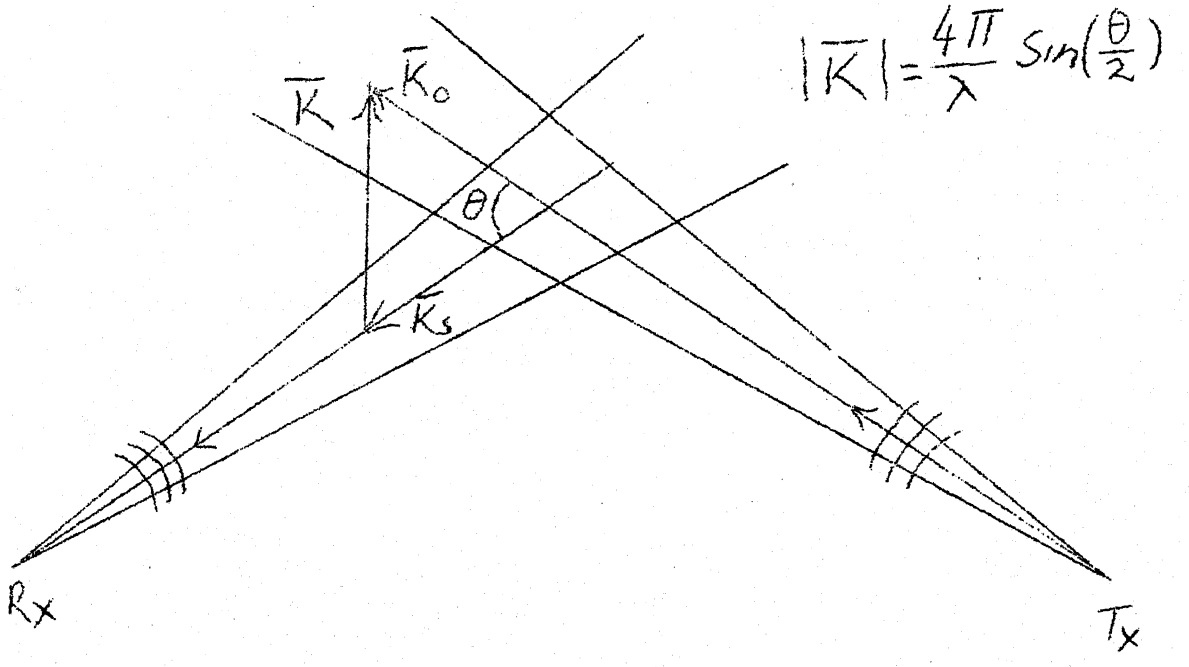

FIG 2.2 SCATTERING VECTOR GEOMETRY

2.2 Common volume scanning:

There are five basic scan types available for effective mapping of the common volume through space (Lammers, 1970). These are:

(1) Vertical Scan. The common volume is scanned in height above a fixed position on the surface of the earth. If P (center of the common volume) is defined by the co-ordinates X_P, Y_P and height H above the surface of the earth, then this scanning technique corresponds to keeping X_P, Y_P constant. This does not change the direction of $\bar{K}$, though its magnitude varies.

(2) Horizontal layer scan along path. The common volume is scanned in a plane parallel to the great circle plane at a fixed height. It corresponds to constant Y_P and H, but changing X_P.

(3) Horizontal scan transverse to the path. This is essentially the same as (2) above except that it is in a plane perpendicular to great circle plane. It corresponds to keeping X_P and H constant and varying Y_P.

(4) Constant scatter angle scan. In a fixed plane containing path terminals, by varying the height above the earth's surface and its position on the surface, the common volume is swung in the space in such a way that the

scattering angle is kept constant. This corresponds to keeping Y_P and $\alpha_{VT} + \alpha_{VR}$ constant. The scatter position movements in the space do not change $\bar{K}$. It can be used to determine spatial inhomogeneities.

(5) Circular scan transverse to the path. It is same as (4) but is in a plane perpendicular to the great circle plane. In this scan the scattering vector $\bar{K}$ changes direction with no change in the magnitude.

Out of these scan types, those at serial No. (1), (2) and (3) are used in order to completely map the common volume and for determination of the tropospheric structures.

2.3 Coordinate Systems; Reference and Local:

Consider Fig. 2.3. The great circle plane is defined in the usual manner by the transmitter T_X, receiver R_X and C the center of the earth. The following assumptions are made for the purposes of analysis.

(a) A corrected radius of the earth (=4/3 Actual radius R) along the great circle path is used in order to compensate for the average decrease in the refractive index value with increase in height. Thus earth is assumed to be a sphere of 4/3 R radius. The values of correction factor

k considering the refractive gradient over Delhi region averaged over a period of 12 months comes to $\frac{4}{3.28}$. However, for computation purpose $k = \frac{4}{3}$ recommended by CCIR for standard atmosphere has been used.

(b) The transmitter and receiver antennas are assumed to be located on the surface of the earth.

Let T_X (X_T, Y_T, Z_T) and R_X(X_R, Y_R, Z_R) be the local co-ordinate systems at transmitter and receiver respectively. Then from Fig. 2.3

$2D$ = path length

T_X = (-D; 0;0) with X,Y,Z as the reference

R_X = (D; 0;0) co-ordinates system

The mid path height H_o of earth's surface above X-Y plane would be

$$H_o = \frac{4}{3} R - \left[\left(\frac{4}{3}R\right)^2 - D^2 \right]^{1/2}$$

Assuming $D \ll \frac{4}{3} R$, it can be simplified as

$$H_o \simeq \frac{D^2}{2\left(\frac{4}{3}R\right)} \qquad (2.5)$$

Let a point P (assumed center of common volume) be defined with coordinates (X_P, Y_P, Z_P). The height of earth's surface above X-Y plane with reference to point P is

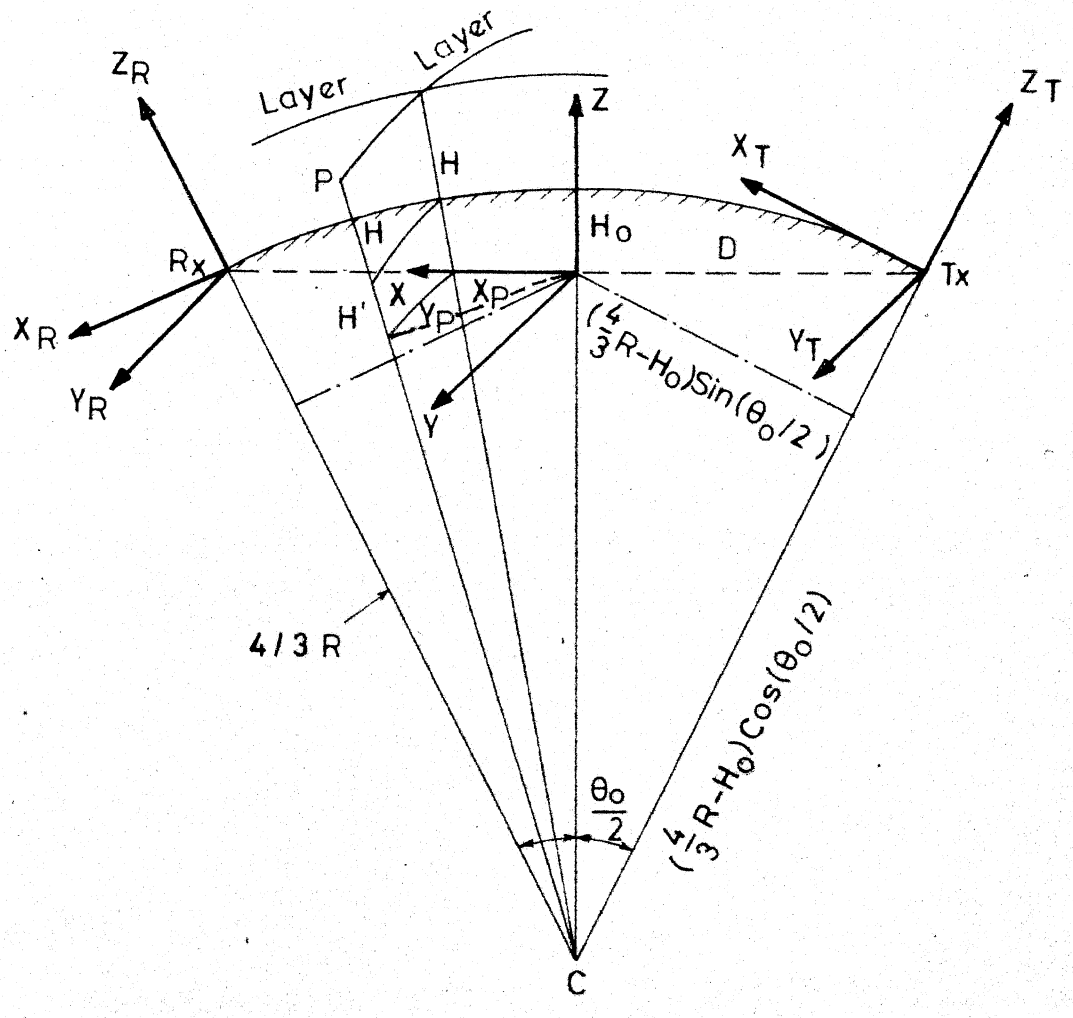

FIG. 2.3 COORDINATE TRANSFORMATION FROM REFERENCE TO LOCAL.

$$H' = \frac{4}{3} R - \left[\left(\frac{4}{3} R - H_o \right)^2 + X_P^2 + Y_P^2 \right]^{1/2}$$

with $X_P^2 + Y_P^2 \ll \frac{4}{3} R$, it reduces to

$$H' = \frac{4}{3} R - \left(\frac{4}{3} R - H_o \right) \left[1 + \frac{X_P^2 + Y_P^2}{2\left(\frac{4}{3} R - H_o \right)^2} \right]^{1/2}$$

or $$H' \simeq H_o - \frac{X_P^2 + Y_P^2}{2\left(\frac{4}{3} R - H_o \right)}$$

But $H_o \ll \frac{4}{3} R$, which can be neglected in the denominator

$$H' \simeq H_o - \frac{X_P^2 + Y_P^2}{2\left(\frac{4}{3} R \right)} \qquad (2.6)$$

H' represents the radial distance of earth's surface from X-Y plane. But because $X_P, Y_P \ll \frac{4}{3} R$, it can be assumed to be the surface height.

Any arbitrary scatter position in an actual link can be referenced by its surface distance from the mid path point, along and across the great circle plane and its height above the surface of the earth, H. This corresponds to X_P, Y_P, Z_P $(= H' + H)$ in (X,Y,Z) co-ordinate system.

An angular rotation of $\left(-\frac{\theta}{2}\right)$ for (X_T, Y_T, Z_T) and of $\left(+\frac{\theta}{2}\right)$ for (X_R, Y_R, Z_R) is required for reference of central coordinate system (X,Y,Z) to the local coordinate system (Fig. 2.3). This rotation yields

$$X_T = X \cos\left(\frac{\theta_o}{2}\right) + Z \sin\left(\frac{\theta_o}{2}\right)$$

$$Y_T = Y$$

$$Z_T = Z \cos\left(\frac{\theta_o}{2}\right) - X \sin\left(\frac{\theta_o}{2}\right)$$

and

$$X_R = X \cos\left(\frac{\theta_o}{2}\right) - Z \sin\left(\frac{\theta_o}{2}\right)$$

$$Y_R = Y$$

$$Z_R = Z \cos\left(\frac{\theta_o}{2}\right) + X \sin\left(\frac{\theta_o}{2}\right) \qquad (2.7)$$

Substitution of Z in terms of H, H_o and R in (2.7) gives the local coordinates in terms of reference co-ordinates as

$$X_T = X \cos\left(\frac{\theta_o}{2}\right) + \left(\frac{4}{3}R + Z - H_o\right) \sin\left(\frac{\theta_o}{2}\right)$$

$$Y_T = Y$$

$$Z_T = \left(\frac{4}{3}R + Z - H_o\right) \cos\left(\frac{\theta_o}{2}\right) - X \sin\left(\frac{\theta_o}{2}\right) - \frac{4}{3}R$$

and

$$X_R = X \cos\left(\frac{\theta_o}{2}\right) - \left(\frac{4}{3}R + Z - H_o\right) \sin\left(\frac{\theta_o}{2}\right)$$

$$Y_R = Y$$

$$Z_R = \left(\frac{4}{3}R + Z - H_o\right) \cos\left(\frac{\theta_o}{2}\right) + X \sin\left(\frac{\theta_o}{2}\right) - \frac{4}{3}R$$

(2.8)

2.4 Elevation and Azimuthal angles:

From the local coordinates of the transmitter and receiver locations (Fig. 2.1) for the given scatter geometry, the elevation and azimuthal angles are

$$\alpha_{HT} = \text{Transmitter azimuthal angle} = \text{Arctan}\left[\frac{Y_T}{X_T}\right]$$

$$\alpha_{VT} = \text{Transmitter elevation angle} = \text{Arctan}\left[\frac{Z_T}{(X_T^2 + Y_T^2)^{1/2}}\right]$$

$$\alpha_{HR} = \text{Receiver azimuthal angle} = \text{Arctan}\left[\frac{Y_R}{X_R}\right]$$

$$\alpha_{VR} = \text{Receiver elevation angle} = \text{Arctan}\left[\frac{Z_R}{(X_R^2 + Y_R^2)^{1/2}}\right]$$

(2.9)

CHAPTER III

COMMON VOLUME ENVIRONMENTS

3.1 Ray Path considerations with Diffraction effects:

For evaluating any troposcatter link design, the detailed knowledge of the atmospheric structures and its effects on the signal passing through it is very essential. The signal ray which passes through the atmosphere suffers any or all of the following

a) Scattering
b) Reflection
c) Refraction

Besides these, the phenomenon of diffraction affects the signal level considerably under certain conditions. The diffraction in a transhorizon path such as troposcatter link occurs in two ways.

i) Diffraction around a smooth spherical earth's surface.

ii) Knife edge diffraction

The diffraction over a smooth homogeneous earth may be determined by the first term of the Vander Pol - Bremmer series (Bremmer, 1949). Certain graphical methods are also known for the determination of signal attenuation in the diffracting regions for both horizontal and vertical

polarization and for any combination of surface conductivity, permittivity ϵ, frequency of operation 'f', distance between terminal points 2D and antenna heights. However the diffraction effects are pronounced only within the distances upto which the diffracted signal is comparable with the scattered signal. The distance beyond the radio horizon at which the scattered and diffracted signals are equal is given by (Chisholm, 1956).

$$d = 65 \left[\frac{0.1}{f_{GHz}} \right]^{1/3} \text{ Km} \qquad (3.1)$$

For Kanpur-Nainital link operating at f = 2.1 GHz.

$$d = 23.5 \text{ Km}$$

Thus we can say that for our link, for distances greater than 23.5 Kms beyond the radio horizon, the scattered field will dominate and hence diffraction effects would be neglected.

In case of knife edge (defined as sharply defined obstacles opaque to and placed in the way of radio waves) the diffraction effects are significant only if the common volume is in very close vicinity of such an obstacles. In such a case Fresnel-Zone clearance from the obstacle top is to be considered (Dalukhanov, 1971).

For Kanpur-Nainital link, there is no such obstacles on the way and hence diffraction is not possible.

3.2 Ray Path considerations and Common Volume Geometry:

The propagation of radio waves through the atmosphere may encounter monotonically decreasing refractivity and/or some abrupt changes in the refractive index with the increasing height. In the first case normal bending of rays due to changes in refractivity can be approximated by the use of modified effective radius of earth. The bending of rays can also be calculated by simple application of Snell's law. But in the second case, if there is sufficient abrupt change in the variation of the refractive index with height (and some times with distance as well) stratification of the atmosphere is said to take place at that height. The stratifications or layers reflect a substantial amount of radio energy at the elevations and frequencies of interest. The reflection co-efficient of the layers decreases with increase in the grazing angle or frequencies.

In the presence of layer structures, the signal strength is expected to be larger than for a well mixed troposphere. The results expected are as shown in Fig. 3.1 (Fengler, 1971).

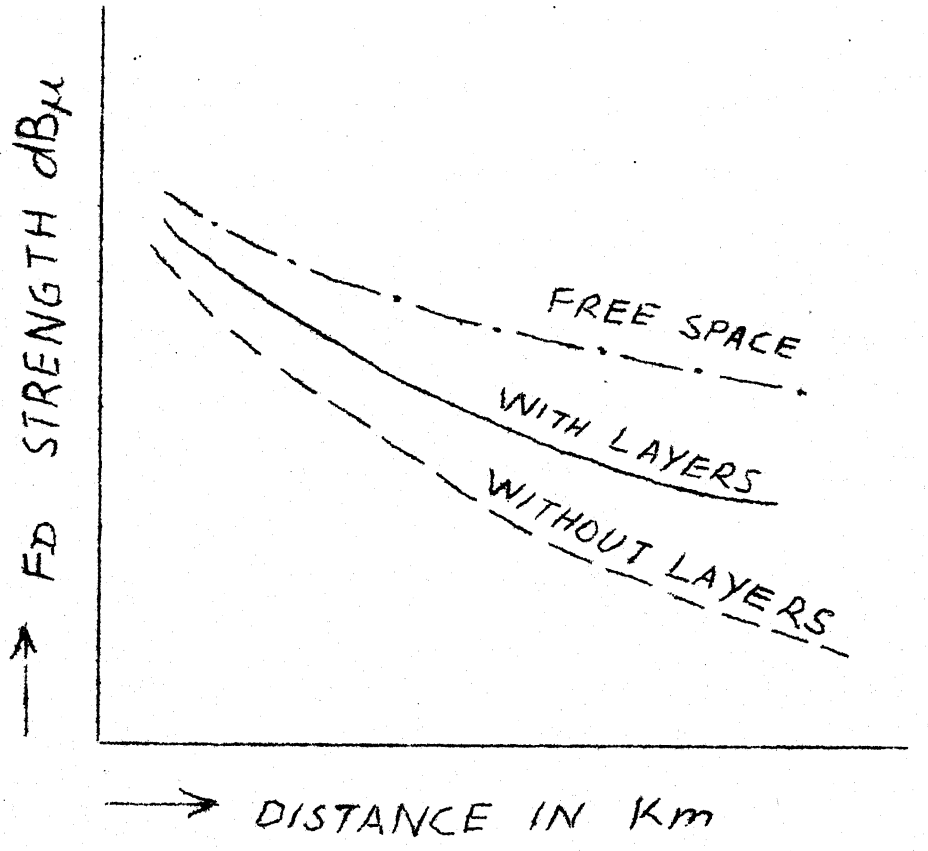

FIG 3.1 RELATIVE SIGNAL STRENGTHS

The signal strengths have also been correlated with the occurance and nature of layers through 'k' diagrams, 'k' being the effective radius of the earth factor (Fig. 3.2). The k-diagrams are the k-profile with height. It is seen that the value of k increases to about 7.3 from its normal values of 4/3 at a height of about 1 Km above sea level. It remains unaltered upto about 1.5 Km height when it again comes to its normal value. This sudden increase in k value provides necessary condition for super-refractive layer (when dN/dh lies between -100 N to -157N, N being refractivity) (Mitra, 1975).

The common volume of the Kanpur-Nainital link is located in a height range of 1.8 Km to 4.6 Km. Therefore the recommended value of k ($= \frac{4}{3}$) is used.

Although there is not much of a correlation between the field strength and k alone, for values of $k > 1.6$, improvement is obtained by correlating field strength with a factor k* which includes the height and thickness of the layers (Marquart, 1970). It is defined as

$$k^* = k - a \frac{h_m - h}{1000_m} - \frac{d.b}{100_m} \qquad (3.2)$$

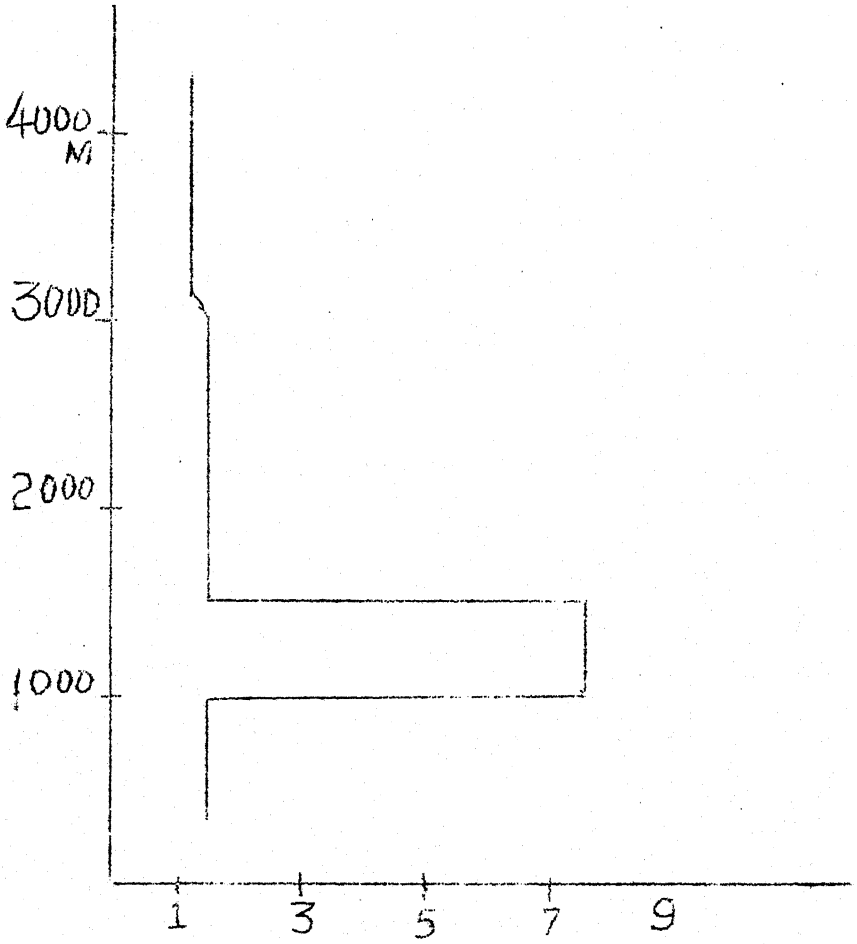

FIG 3.2 k- PROFILE

where

'a' = a parameter representing height influence

b = a parameter representing the layer thickness influence

h = actual height (of layer)

d = actual thickness (of layer)

h_m = the height in which the layers have maximum efficiency.

Further, scattered power is a function of θ, in that it depends on $(\sin \frac{\theta}{2})^{-p}$, 'p' being power index. The value of 'p' may lie between 2 and 5. The value generally accepted and used is $\frac{11}{3}$ (Tatarski, 1961). Thus any increase in scattering angle θ will increase the height and decrease the magnitude of common volume. The increase in the height of common volume tends to decrease the intensity of turbulence causing weak scattering, since $\overline{\Delta n^2}$, mean square fluctuations in the refractive index, decrease with height. Hence one has to compromise in keeping the beams as low as possible and gaurd against the obstacle blockade.

For Kanpur-Nainital link, the axes of antennas are parallel to the $\angle^{\text{tangents}}$ to the earth's surface at the point of antenna mounting instead of pointing towards horizon. The geometry of the link is given in Fig. 3.3.

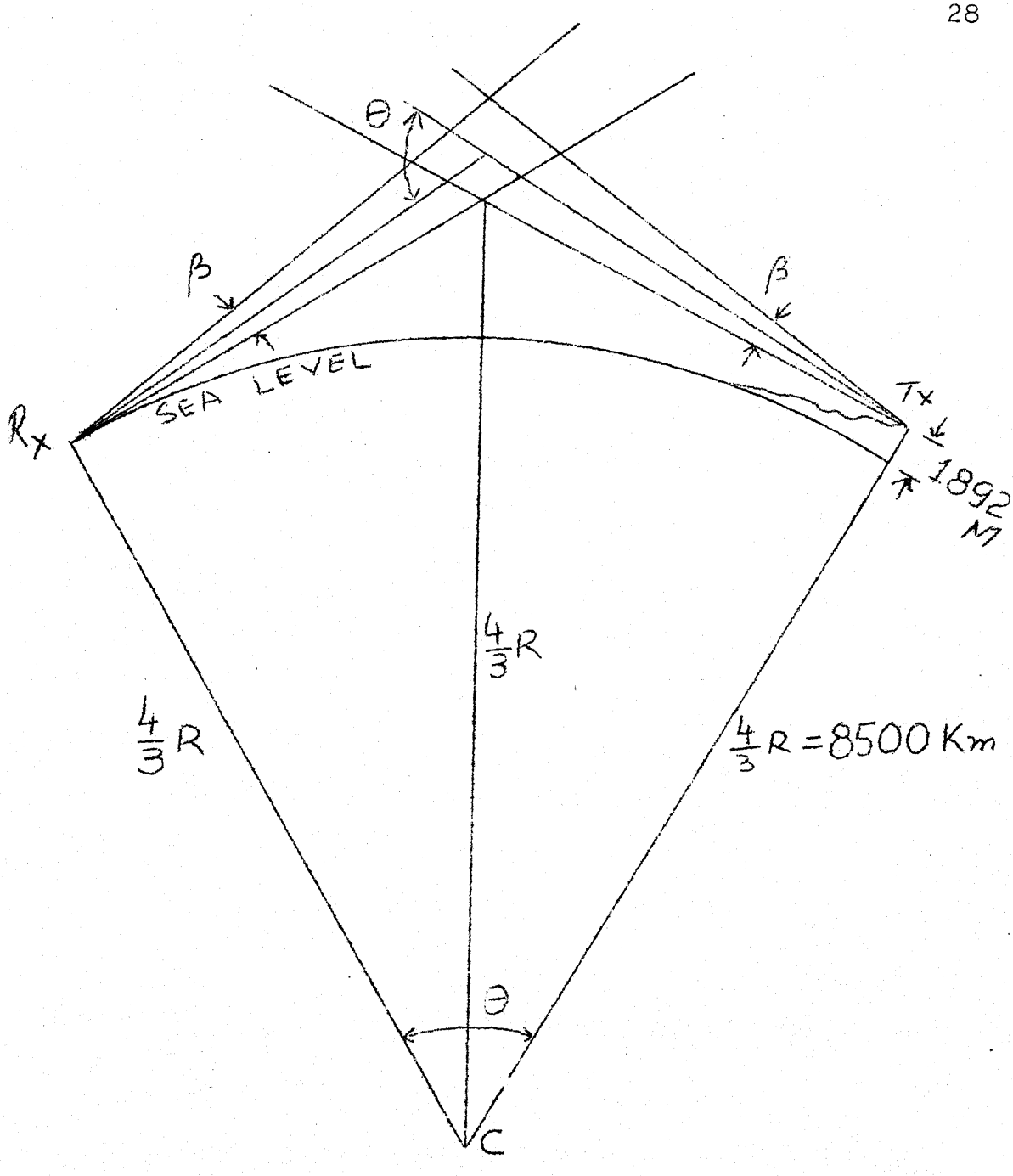

FIG 3.3 LINK GEOMETRY

The heights of transmitter and receiver antennas above the mean sea levels are 1892 meters and 145.8 meters respectively, which are very small as compared to effective radius of the earth ($= \frac{4}{3} R = 8500$ Km). Hence these are neglected and the antennas are assumed to be located at the surface of the earth. The modified link geometry therefore would be as in Fig. 3.4.

All the points located above tangent planes L_2 and L_4 (Fig. 3.4) have the property of being simultaneously seen from the terminals of the link. The collection of these points within the troposphere contained in the area bounded by the tangent planes L_1, L_2, L_3 and L_4 is called scatter volume or common volume. This is true, however for narrow-beam antennas. In the case of antennas having larger antenna beam widths, the common volume is not dependent on the tangent planes but on the $(\theta)^{-p}$ power dependence.

3.3 Link parameters for Kanpur-Nainital Link:

Height of Transmitting antenna above ground level
= 14 ft or 4.3 m.

Height of Transmitting antenna above mean sea level
= 1892 m

Height of Receiver antenna above ground level
= 60 ft. or 18.4 m

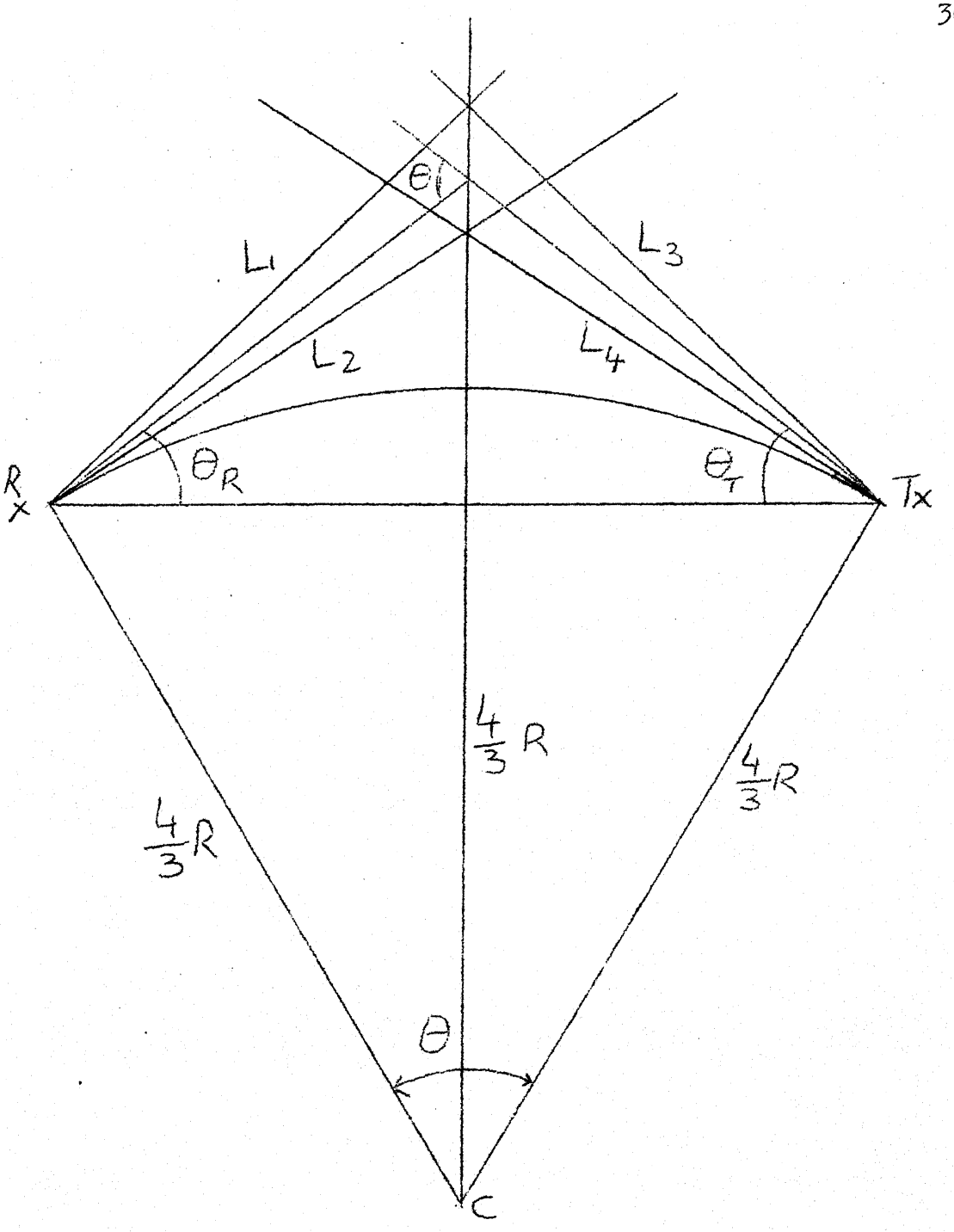

FIG 3.4 MODIFIED LINK GEOMETRY

Height of Receiver antenna above mean sea level
= 145.8 m

Distance between transmitter and receiver
= 330 Km.

3 dB beam widths of receiver and transmitter antennas = =0.95 degrees = 16.6 MR

Maximum antenna gain G_o = 42 dB.

3.4 Estimation of common volume:

In the study done by Gupta(1973), the common volume for Kanpur-Nainital link has been calculated approximately. The antenna cone tangent planes are assumed to constitute rhombic common volume geometry. The parameters such as θ, mean height of common volume calculated as above have further been used for study of troposcatter signal characteristics based on random layered scatter model (Bassi, 1974) and for determining the 'Rake' characteristics of the link (Rama Rao,1975).

But because of the assumptions of narrow horizontal layers that partially fill the common volume, backed by the experimental observations (Lammers, 1970) the detailed size of the common volume is required to be calculated. For this purpose consider Figs. 3.5 and 3.6. These give the general orientation of the scatter systems

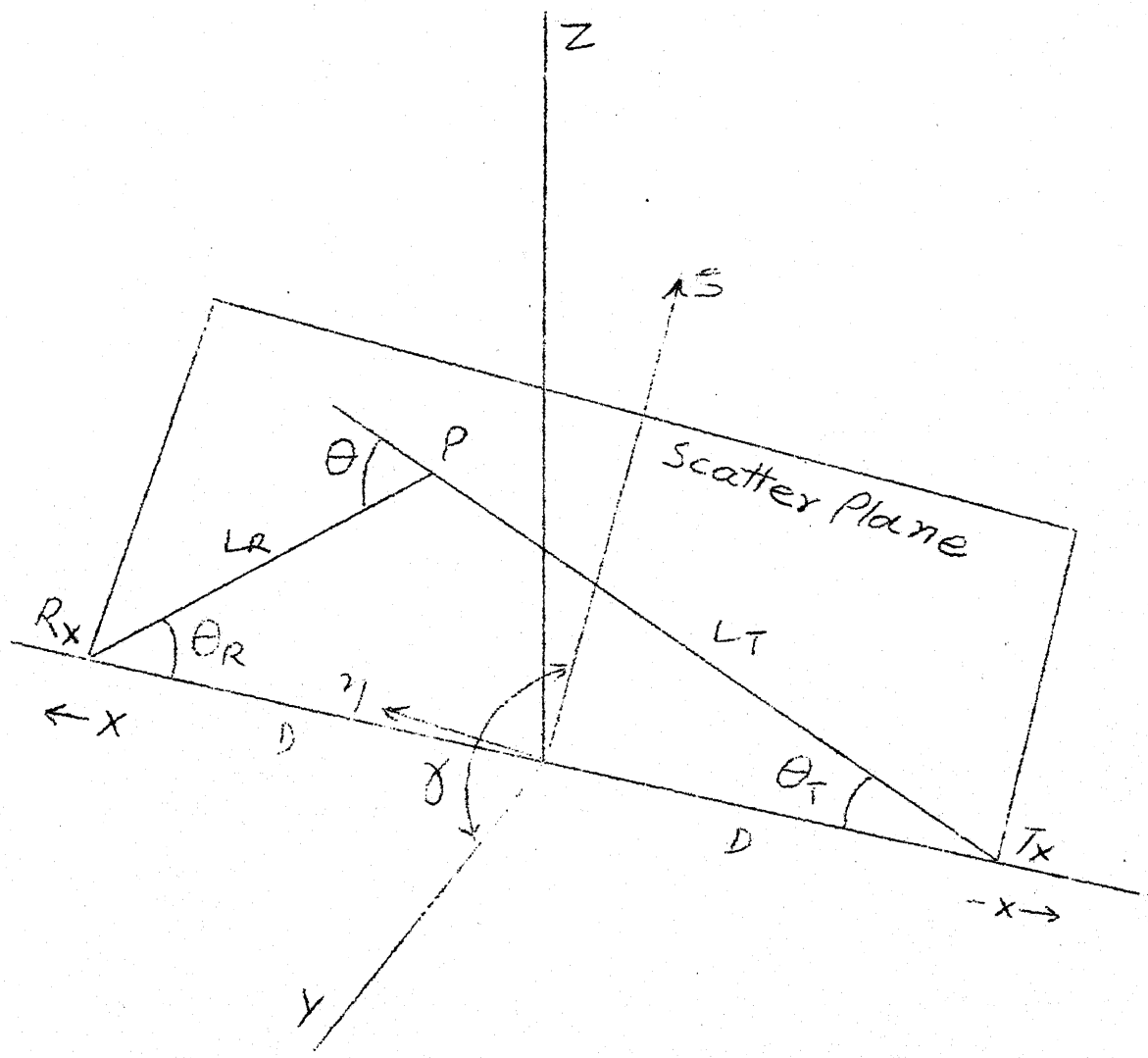

FIG 3.5 GENERAL ORIENTATION OF SCATTER SYSTEM WITH SCATTER PLANE

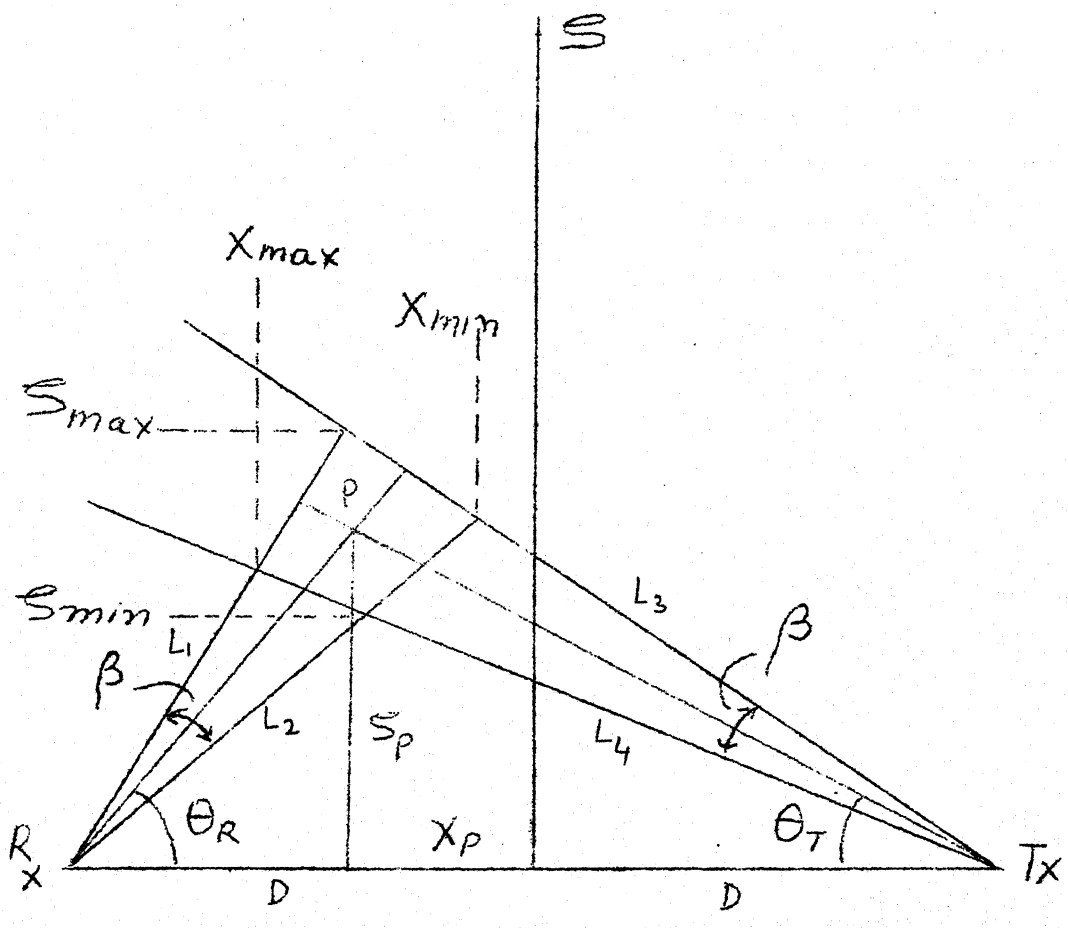

FIG3.6 FORWARD SCATTER GEOMETRY

with scatter plane and forward scatter geometry which are used for determination of the scatter volume limits to be used in the integration.

A mid path cartesian system (X,Y,Z) is chosen for basic reference such that R_X = (D; 0; 0) and T_X = (-D; 0; 0). A scatter plane is assumed to be hinged to the X-axis (Fig. 3.5). This plane is defined as a plane containing R_X, T_X and scatter point P, the center of the common volume .

For the sake of convenience, a subsidiary set of coordinates such as (X, η, ξ) are chosen for the estimation of the common volume limits. The subsidiary coordinate system chosen is such that its origin coincides with the central reference coordinate system (X, Y, Z), with η perpendicular to and ξ within the scatter plane. The transmitter and receiver antennas beams are replaced by cones of equal width. The scatter plane determines the inclination γ of the subsidiary coordinate systems used in the integration process. θ_T and θ_R are the antenna elevation angles in the scatter plane and θ is the scattering angle. In order to provide complete (X, Y,Z) coverage of the scatter volume center point, the γ variations are within the limits as $0 \leq \gamma \leq \pi$

Consider the intersection of the cones on the scatter plane, as L_1 through L_4. The intersection of (L_1, L_4) and (L_2, L_3) determines the X-limits and the intersection of (L_2, L_4) and (L_1, L_3) determines the ζ-limits. Then with the scatter volume center position $P(X_P, \zeta_P)$ on the scatter plane

$$\theta_T = \arctan\left(\frac{\zeta_P}{D+X_P}\right)$$

$$\theta_R = \arctan\left(\frac{\zeta_P}{D-X_P}\right) \qquad (3.3)$$

The tangant planes from L_1 through L_4 would be

$$TR1 = \tan(\theta_R + \beta/2)$$
$$TR2 = \tan(\theta_R - \beta/2)$$
$$TT1 = \tan(\theta_T + \beta/2)$$
$$TT2 = \tan(\theta_T - \beta/2) \qquad (3.4)$$

The linear equations for the planes, thus are

$$\text{For } L_1 \qquad \zeta = TR1\ (D-X)$$
$$\text{For } L_2 \qquad \zeta = TR2\ (D-X)$$
$$\text{For } L_3 \qquad \zeta = TT1\ (D+X)$$
$$\text{For } L_4 \qquad \zeta = TT2\ (D+X) \qquad (3.5)$$

The intersection of these with one another give integration limits on X-ζ plane as

$$X_{min} = \frac{TR2 - TT1}{TR2 + TT1} \cdot D$$

$$X_{max} = \frac{TR1 - TT2}{TR1 + TT2} \cdot D$$

$$\mathcal{S}_{min} = \frac{TR2 \cdot TT2}{TR2 + TT2} \cdot 2.D$$

$$\mathcal{S}_{max} = \frac{TR1 \cdot TT1}{TR1 + TT1} \cdot 2.D \qquad (3.6)$$

For determining η -limits, consider Figs. (3.7) and (3.8). Consider an elementary volume S = $(X, \eta, \mathcal{S})$. Projecting S on X -$\mathcal{S}$ plane S_1 is obtained. Now any plane through S and perpendicular to the transmitter beam direction would intersect PT at S_o. For $\eta > 0$ the intersection of the plane through S and of antenna cone of apex angle $2\beta_T$ indicated by the semi circle of the radius SS_o determines the η -limits.

If L_T is the distance of the scattering point from the transmitter, then considering relative distances

$$ST \leq S_1T \leq S_oT \leq L_T$$

and $$L_T = \left[(D + X)^2 + \mathcal{S}^2\right]^{1/2} \qquad (3.7)$$

Also $$\eta^2 + (S_oS_1)^2 = (SS_o)^2 \qquad (3.8)$$

Further

$$\tan \left[\angle S_oTS_1 + \theta_T\right] = \frac{\mathcal{S}}{D + X}$$

$$\therefore \quad \angle S_oTS_1 + \theta_T = \arctan \left(\frac{\mathcal{S}}{D+X}\right)$$

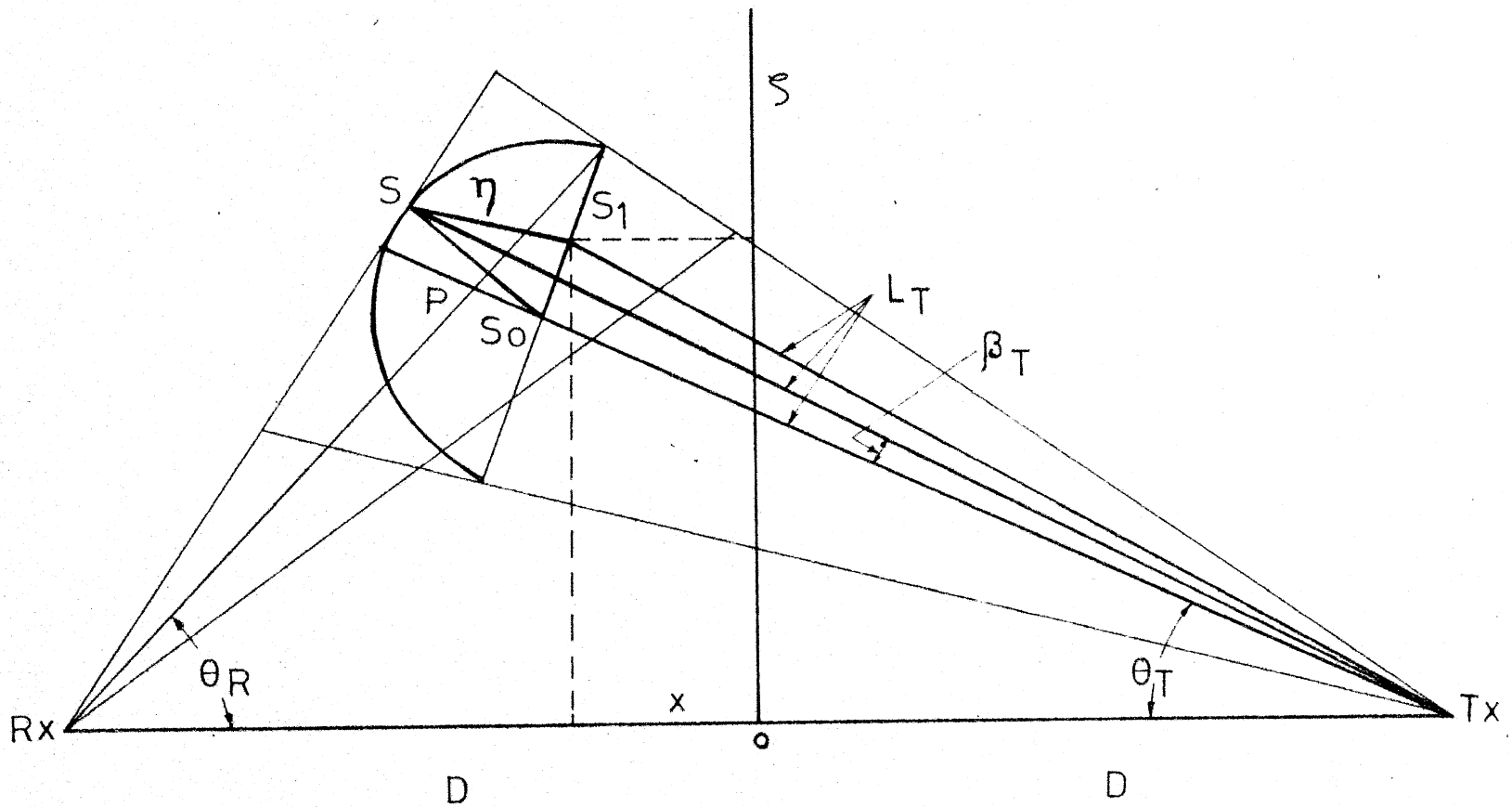

FIG. 3.7 η - LIMITS OF SCATTER VOLUME

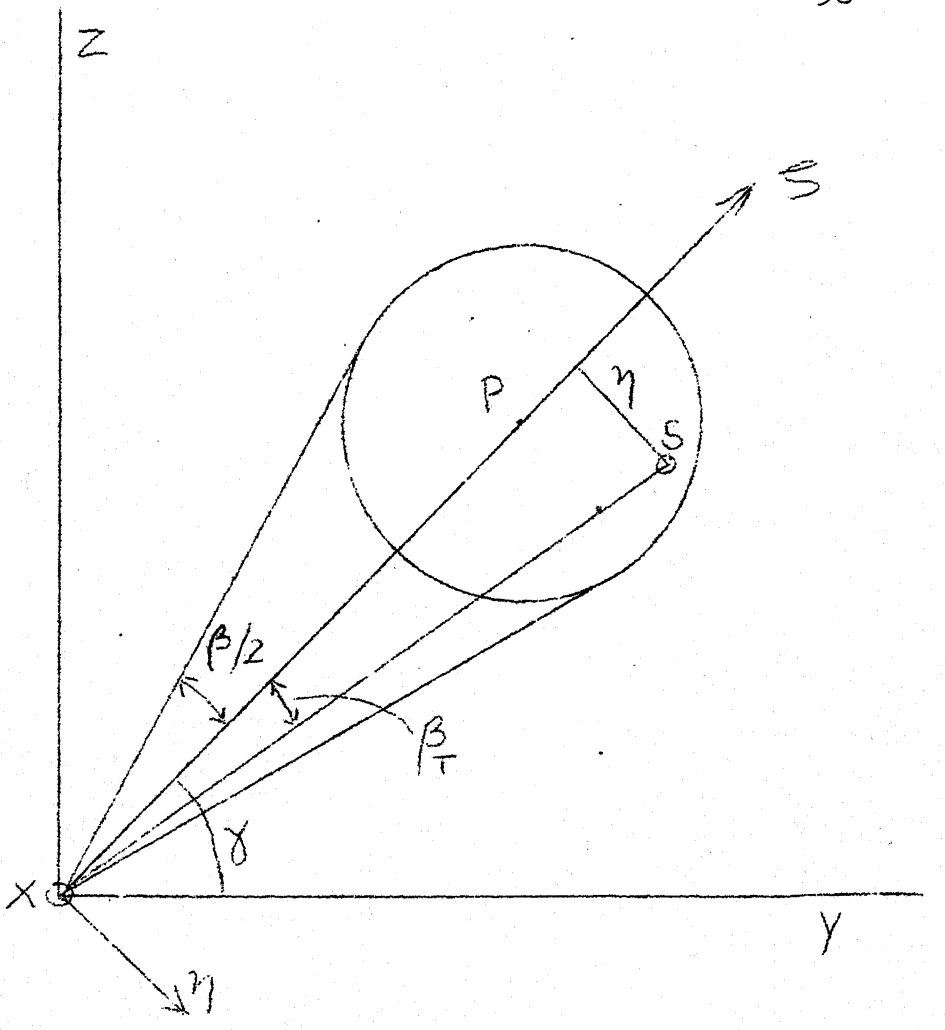

FIG 3.8 DETERMINATION OF η-LIMITS OF INTEGRATION

or $\angle S_o T\, S_1 = \arctan\left(\frac{\varsigma}{D+X}\right) - \theta_T$

$$= \frac{S_o S_1}{L_T}$$

Thus $S_o S_1 = L_T \left(\arctan \frac{\varsigma}{(D+X)} - \theta_T\right)$ (3.9)

Similarly

$$SS_o = L_T \beta_T \tag{3.10}$$

Substituting (3.9) and (3.10) in (3.8)

$$\eta^2 = L_T^2\left[\beta_T^2 - \left(\arctan \frac{\varsigma}{D+X} - \theta_T\right)^2\right] \tag{3.11}$$

Replacing β_T by half antenna beamwidth gives the maximum distance of the transmitter antenna cone above the scatter plane. Thus replacing β_T by $\beta/2$ and substituting (3.7) for L_T in expression (3.11) gives one of the η-limits of the integration as

$$\eta_{T_{max}} = \left\{\left[(D+X)^2 + \varsigma^2\right]\left[\left(\frac{\beta}{2}\right)^2 - \left(\arctan \frac{\varsigma}{D+X} - \theta_T\right)^2\right]\right\}^{1/2} \tag{3.12}$$

In a similar way for the receiver antenna, the η-limits are obtained by replacing θ_T with θ_R, β_T with β_R and substituting expression

$$L_R^2 = (D - X)^2 + \varsigma^2$$

instead of L_T in (3.11) as

$$\eta_{R_{max}} = \left\{\left[(D-X)^2 + \varsigma^2\right]\left[\left(\frac{\beta}{2}\right)^2 - \left(\arctan\left(\frac{\varsigma}{D-X}\right) - \theta_R\right)^2\right]\right\}^{1/2} \qquad (3.13)$$

The limits for negative η values are

$$\eta_{T_{min}} = -\eta_{T_{max}}$$

and $$\eta_{R_{min}} = -\eta_{R_{max}} \qquad (3.14)$$

Thus knowing all the limits the integral can be evaluated using any of the standard integration techniques.

The angular distance of elemental volume from the antenna beam axes is given as

$$\beta_T = \left[\frac{\eta^2}{(D+X)^2+\varsigma^2} + \left(\arctan\frac{\varsigma}{D+X} - \theta_T\right)^2\right]^{1/2} \qquad (3.15)$$

and

$$\beta_R = \left[\frac{\eta^2}{(D-X)^2+\varsigma^2} + \left(\arctan\frac{\varsigma}{D-X} - \theta_R\right)^2\right]^{1/2} \qquad (3.16)$$

The antenna gain functions are, therefore given as

$$G_T = G_o.\mathrm{Exp}\left[-f\,.\beta_T^2\right]$$

and $$G_R = G_o.\mathrm{Exp}\left[-f\,.\beta_R^2\right] \qquad (3.17)$$

where G_o and f are respectively the peak gain and antenna shaping factor. The incremental scatter volume is weighted by

$$G_R\,G_T = G_o^2\,\mathrm{Exp}\left[-f(\beta_R^2 + \beta_T^2)\right] \qquad (3.18)$$

CHAPTER IV

DETERMINATION OF SCATTER POWER

4.1 Brief description of Scatter Theories and Scatter Mechanism:

Three distinct groups of theoretical work have been used to explain the scatter mechanism. These are

(a) Theories based on turbulence (Booker-Gordon)

(b) Mode Theories (Eullinsten etc)

(c) Reflection Theories (Friis, Hog, Crawford)

Each theory has the backing of some reasonable experimental work.

The elements of Booker-Gordon, Villars - Weiskopf's and Tatarski's theories are explained in fair details in the earlier works (Gupta, 1973; Bassi, 1974). The theory of reflection from the infinite flat layers (Friis theory) is discussed in chapter V. Some details of scatter theory based on the work of Gjessing (Gjessing, 1969) are discussed here. This scattering theory determines the fine scale properties of the refractive index structure. The refractive index spectrum is defined as

$$\Phi(\bar{K}) = |\bar{K}|^{-p} \qquad (4.1)$$

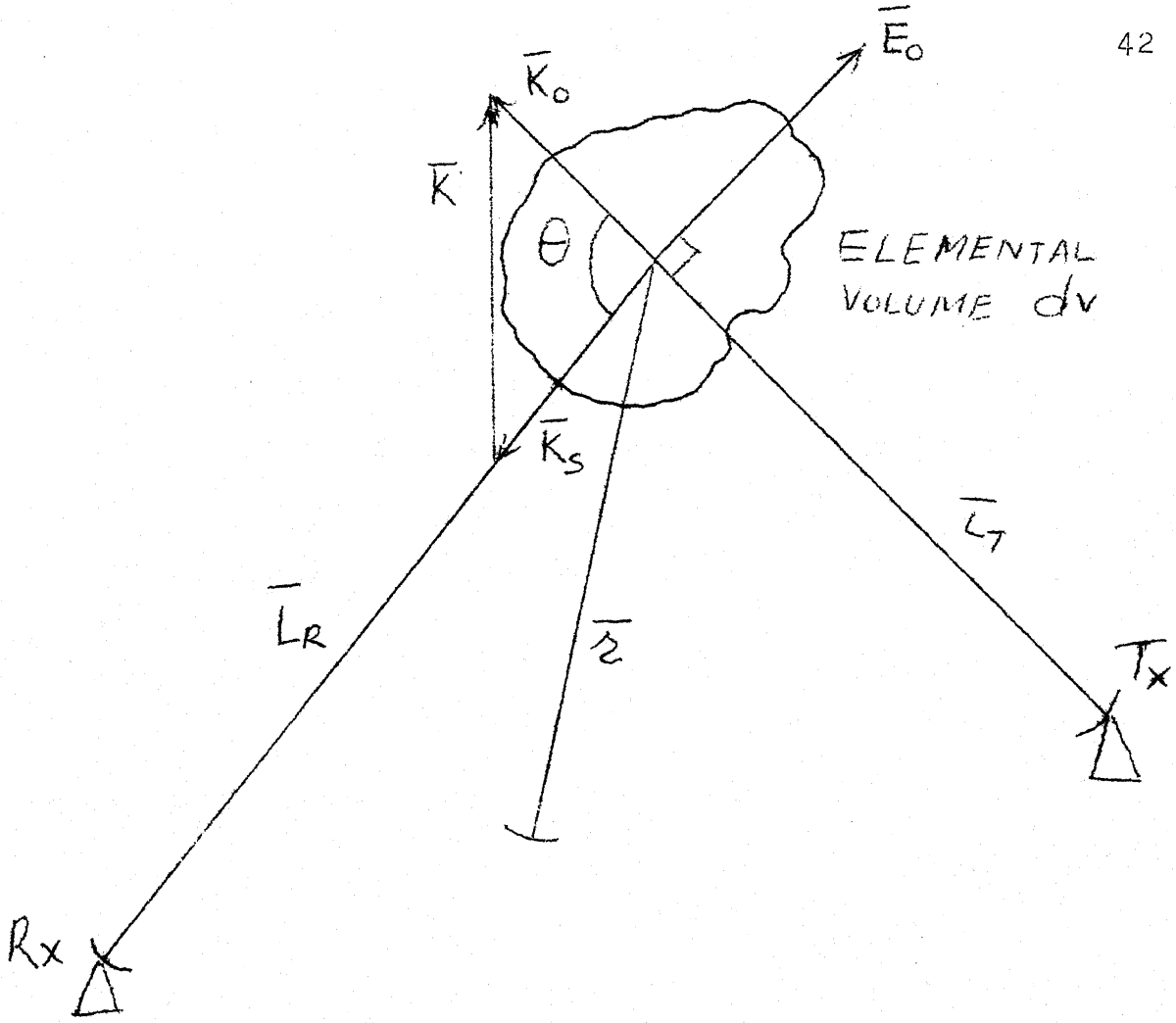

FIG 4.1 SCATTERING FROM ELEMENTAL VOLUME.

where $\bar{K} = \bar{K}_o - \bar{K}_s$; $\bar{K}_o$, $\bar{K}_s$ being wave numbers of incident and scattered fields and θ is the angle between $\bar{K}_o$ and $\bar{K}_s$ (Fig. 4.1), and

$$|\bar{K}| = \frac{4\pi}{\lambda} \sin\left(\frac{\theta}{2}\right) \tag{4.2}$$

Assuming incident wave to be plane and that the linear extent of common volume ($\simeq V^{1/3}$) very small compared to the distances between common volume and the terminal stations, the scattering cross-section is given as (Gjessing, 1969)

$$\sigma(\theta) = \frac{\pi K^4}{2} \Phi(\bar{K}) \tag{4.3}$$

where $\Phi(\bar{K})$ is the spatial power spectrum of refractive index. Thus in general from (4.3) the three dimension spectrum can be expressed as in (4.1). With isotropic refractive index field, the power spectrum of scattered wave is given by

$$P(\theta) \propto \theta^{-p} \tag{4.4}$$

There can be three different cases for scattering mechanism as given below.

Case I

Scattering by homogeneous isotropic turbulence:

In the wave number (K) range corresponding to the inertial sub range, the one directional refractive

refractive index spectrum E(K) can be expressed in terms of turbulence theory as

$$E(K) = \langle \delta\epsilon^2 \rangle_{av} \, l^{-2/3} \, K^{-5/3} \qquad (4.5)$$

where $\langle \delta\epsilon^2 \rangle_{av}$ = standard deviation of permittivity fluctuations

l = input scale

($= \frac{2\pi}{Km}$, Km being wave number for maximum E(K))

E(K), in effect, is one dimensional power spectrum obtained by integration of $\phi(\bar{K})$ over all directions of scattering vector. In case of isotropic medium, it takes the form

$$E(K) = 4\pi K^2 \phi(\bar{K}) \qquad (4.6)$$

This gives the refractive-index spectrum in the inertial sub range as (Gjessing; 1964a)

$$\phi(K) = 0.03 \, C_n^2 \, K^{-11/3} \qquad (4.7)$$

where $$C_n^2 = 5.3 \langle \delta\epsilon^2 \rangle_{av} \, l^{-2/3} \qquad (4.8)$$

= Tatarski's structure function coefficient.

In (4.8), p has been replaced with (-11/3) in accordance with Tatarski's theory of turbulence. Substituting these values in (4.3) gives the scattering cross-section $\sigma(\theta)$ as

$$\sigma(\theta) = 0.03 \, C_n^2 \, \lambda^{-1/3} \, (\sin \tfrac{\theta}{2})^{-11/3} \qquad (4.9)$$

Case II

Scattering from stable region:

Assuming single horizontal layer through which refractive index varies systematically based on the mean temperature mean humidity and mean pressure, the scattered field $\bar{E}_s$ at a distance R from scattering element, under the influence of incident field E_o is given by

$$\bar{E}_s = \frac{K_s^2 \bar{E}_o}{4\pi R} \Lambda(\bar{K}) \qquad (4.10)$$

where $\Lambda(\bar{K}) = \int f(\bar{r}) \exp\left\{-j(K_x x + k_y y + K_z .z)\right\} dx.dy\, dz$

(4.11)

and $f(\bar{r})$ is the space function (Gjessing, 1964a, 1969). But it is assumed that per-mittivity is constant in X and Y direction and changes only in the vertical direction. Then $f(\bar{r})$ can be replaced with $f(z)$ and therefore

$$\Lambda(\bar{K}) = \int f(z)\, e^{-jK_z \cdot z}\, d_z \int e^{-jK_y \cdot y}\, d_y \int e^{-jK_x \cdot x}\, .dx \qquad (4.12)$$

In (4.12) the integrals with x and y arguments are the Fourier representation of the delta function. Thus

$$\Lambda(\bar{K}) = \int f(z)\, e^{-jK_z \cdot z}\, dz . \delta(K_y).\delta(K_x) \qquad (4.13)$$

The function $A(\bar{K})$ and hence $\bar{E}_s$, therefore vanish unless both K_x and K_y are zero. This means that for $\bar{E}_s$ to exist, $\bar{K}$ must be normal to the layer boundary. In this case scattering cross section is given by the product of $A(\bar{K})$ with its complex conjugate as

$$\sigma(\theta) = \frac{\pi K^2}{2} \left| \int f(z)\, e^{-jK_z \cdot z} \cdot dz \right|^2 \qquad (4.14)$$

Case III

Scattering from strong turbulent layers:

The intense turbulence affecting propagation, in this case, is confined to the horizontal layers of very limited vertical extent. The layer boundaries will not be smooth in terms of λ . But these layers are associated with large degree of local stability. There are therefore two factors contributing to the scattered power:

(a) Scattering from mean profile as discussed in case II above.

(b) Super imposed on this, the scattering due to random refractivity fluctuations caused by intense turbulence.

The resultant scatter field is sum of the two and is given by

$$\sigma(\theta) = .03\, C_n^2\, \lambda^{-1/3}\, (\sin\theta/2)^{-11/3} + \frac{\pi K^2}{2} \left| \int f(z)\, e^{-jK_z \cdot z} \cdot dz \right|^2 \qquad (4.15)$$

The relative importance and hence contribution of the two terms depends on

(a) relative magnitude of r.m.s. random refractive fluctuations and degrees to which refractive index varies through the layer,

(b) thickness of the layer in relation to the quantity $\lambda/\sin\theta$ and

(c) radio wave length λ in relation to input scale 'l' of turbulent field.

If the layer thickness is comparable with scale $\frac{2\pi}{K}$ which contributes to scattering at a particular λ and a particular θ, then the layers have pronounced effect.

The power received at the receiver antenna may be expressed

$$P_R = P_s + P_d$$

where P_s is power due to scattering by turbulence and P_d is the power due to glints or facets (the glints/facets are the sharp boundary variations within the common volume). The refractive index modulus M(= N+157) gradient completely describes the value of P_s. In case of narrow beam antenna it is given by (Mitra, 1975).

$$P_s = P_{fs}\ 0.76.10^{28}.\ C_n^2\ .\left(\frac{dM}{dh}\right)^{-14/3}.(2D)^{-11/3} \cdot \lambda^{-1/3} \cdot \beta^3 \qquad (4.16)$$

where P_{fs} is free space propagation power, 2D is the distance between T_X and R_X, and β is antenna beam width in radians.

In case of P_d, the troposphere is assumed to be completely mixed excepts for glints. This can be characterised by an equivalent or effective reflection area A_e. The geometrical area of glints is assumed to be very small as compared to first Fresnel zone clearance but is large as compared to the wave length. In such a case P_d is given by (Mitra, 1975)

$$P_d = P_{f.s.}\ \frac{4}{\pi D^2} \int_V N \cdot A_e \cdot dv \qquad (4.17)$$

In cases where random fluctuations in the refractivity follow the inertial sub range $K^{-5/3}$ law (meaning there-by that $\Phi(K)$ is proportional to the value of $K^{-11/3}$), the dependence of received power on the scattering angle is

$$P(\theta) \propto (K) \cdot V \qquad (4.18)$$

But for narrow beam antennas

$$V \propto \theta^{-1}$$

and $$(K) \propto \theta^{-11/3}$$

$$\therefore \quad P(\theta) \propto \theta^{-\left[\frac{11}{3}+1\right]} \tag{4.19}$$

This is true for scattered power. In case of specular reflection, assuming linear decrease of Δn over the height interval Δh, the power reflection coefficient is given by

$$|\rho^2| = \left| \frac{\Delta n}{2 \sin^2(\frac{\theta}{2})} \cdot \left(\frac{\sin X}{X} \right) \right|^2 \tag{4.20}$$

where X is defined as

$$X = \frac{2\pi \Delta h}{\lambda} \sin\left(\frac{\theta}{2} \right)$$

The two limitting cases depending on the size of the layer are

(i) Infinitely thin layer ($\Delta h \to o$). In this case

$$|\rho^2| = \left| \frac{\Delta n}{2 \sin^2(\frac{\theta}{2})} \left\langle \frac{\sin X}{X} \right\rangle \right|^2$$

which gives

$$P(\theta) \sim \theta^{-4} \tag{4.21}$$

(ii) Infinitely thick layer ($\Delta h \to \infty$). The angular spectrum in this case is given by

$$|\rho^2| = \left| \left\langle \frac{dn}{dh} \frac{\lambda}{\sin^3(\frac{\theta}{2})} \right\rangle \right|^2$$

which gives

$$P(\theta) \sim \theta^{-6} \qquad (4.22)$$

4.2 Scatter Integral and its Evaluation:

The forward scattered power P_R arriving at the receiving end is obtained by integrating over the common volume V and is given by (2.1), where $\sigma(\theta)$ is the scattering cross section (also called reflectivity of the turbulent medium per unit volume). In one form of the many representations of Tatarski's theory, it is defined by (4.9) considering polarisation factor also, $\sigma(\theta)$ takes the form of

$$\sigma(\theta) = 0.38\, C_n^2\, \lambda^{-1/3} \left(\sin \frac{\theta}{2}\right)^{-11/3} \cdot \sin^2 \chi \qquad (4.23)$$

where χ is the angle between the electric field vector of transmitted ray at the scatter point and scattered ray towards the receiver. $\sin^2 \chi$ accounts for the polarisation effects. Expression (4.23) considers isotropic spectrum given by eqn (2.3).

While considering narrow beam forward scatter system, C_n^2 and $\sin^2 \chi$ are taken as constant for integrating over the common volume (Lammer, 1972).

G_T, G_R, L_T, L_R and Θ are all considered variable for this purpose. Substituting (4.23) in (2.1) gives the scatter integral

$$P_R = 1.91 \cdot 10^{-4} \cdot P_T \cdot \lambda^{5/3} \cdot C_n^2 \cdot \sin^2\chi \int_V \frac{G_T \cdot G_R}{L_T^2 L_R^2 (\sin\frac{\Theta}{2})^{11/3}} dv \qquad (4.24)$$

This gives theoretical value of P_R . When it is compared with the expreimental observations there exists some descrepency. This is due to the fact that

i) The troposphere cannot be considered turbulent throughout its extent and

ii) significant scattering takes place over a limited region only.

Based on the study of data from a large number of troposcatter links, the region of significant scatter in the troposphere can be assumed to be a thin layer (Hardy et.al, 1966 ; Crane, 1968). However there may be more than one layer affecting the scattering from the common volume. High resolution radars used to probe the troposphere have suggested that a horizontal layer of vertical extent of 100 meters is representative of the actual conditions.

In order to solve scatter integral (4.24) the integration is carried out over the auxillary coordinate system (x, η, ζ). The boundary limits of bounding surfaces x, η, ζ are determined as per (3.6), (3.12) and (3.13) Even after determination of boundary limits, because of extremely complex nature of the common volume no analytical solution of scatter integral (4.24) is available. It is therefore solved numerically. For this purpose a limitting surface of $(X_{max} - X_{min})$ and height $(\zeta_{max} - \zeta_{min})$ is chosen in $x - \zeta$ plane for any arbitrary scatter plane inclination γ. If a small elemental volume $(dx\, d\eta\, d\zeta)$ within this surface is taken, it will contribute to the scattering only if its height above the scatter plane lies within the transmitter and receiver antenna cones. Whenever this condition is met by a particular volume element, it indicates the extent of the scatter integral involved. For obtaining received power, the above is to be weighted, with reference to the scatter plane, by appropriate gain functions G_R, G_T and L_R^2, L_T^2, with θ dependency as $(\sin \frac{\theta}{2})^{-11/3}$. Depending on the position of scatter volume and that of the scatter plane inclination γ with relation to great circle plane, a height above the surface of the

earth is attached to above. All incremental volumes within the common volume are, in this way, assembled together into sets of height intervals for any arbitrary scatter plane inclination.

There is a change of coordinate system from reference to auxillary (x, η, ζ) in order to achieve integration. For this purpose consider Fig. 4.2 which shows arbitrarily chosen general location of the scatter point P.

It is seen that

$$Z_P = PA + AB$$

and $PA = -\eta \cos\gamma$, $AB = DC = \zeta \sin\gamma$.

$$\therefore \quad Z_P = \zeta \sin\gamma - \eta \cos\gamma \tag{4.25}$$

Similarly

$$Y_P = DC - BC \ (= AD) \text{ or}$$

$$Y_P = \zeta \cos\gamma + \eta \sin\gamma \tag{4.26}$$

Solving (4.25) and (4.26) for η and ζ gives the values of anxillary coordinate systems in terms of central reference coordinate system as

$$\eta = Y_P \sin\gamma - Z_P \cos\gamma$$

$$\zeta = Y_P \cos\gamma + Z_P \sin\gamma \tag{4.27}$$

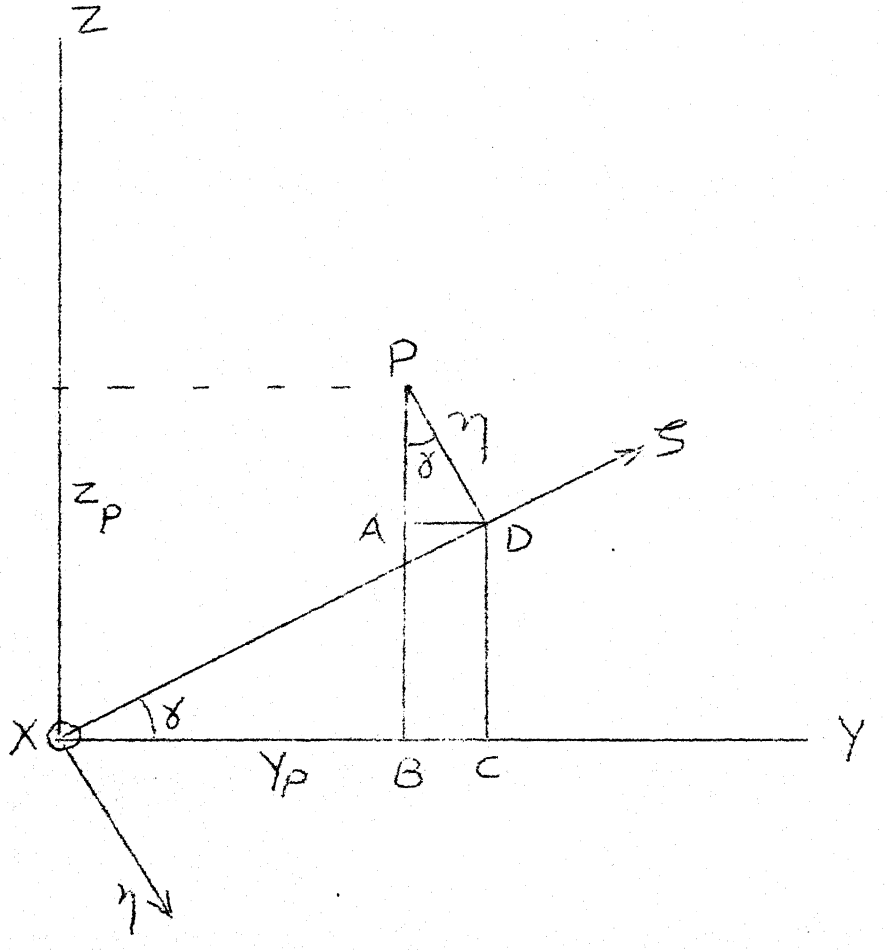

FIG 4.2 AUXILLARY COORDINATES

For ascertaining the height of any scatter element above the surface of the earth consider Fig. 4.3 where 's' shows the thickness of the scattering layer. Then

$$\tan \gamma = \frac{Z_P}{Y_P}$$

and $$Z = S \sin \gamma - \eta \cos \gamma$$

Substituting for $\sin \gamma$ and $\cos \gamma$ in terms of Y_P and Z_P gives

$$Z = S \cdot \frac{Z_P}{(Y_P^2 + Z_P^2)^{1/2}} - \eta \cdot \frac{Y_P}{(Y_P^2 + Z_P^2)^{1/2}}$$

or $$Z = \frac{S.Z_P - \eta.Y_P}{\left[Y_P^2 + Z_P^2\right]^{1/2}} \qquad (4.28)$$

In the actual computer processing all elementary scatter volumes are referenced by their height Δh with reference to the center of the common volume as

$$\Delta h = Z - Z_P \qquad (4.29)$$

The approximate height of the scatter element above the earth's surface is

$$H = Z - H_o$$

or $$H = \frac{S Z_P - \eta Y_P}{\left[Y_P^2 + Z_P^2\right]^{1/2}} - \frac{(D\ )^2 - X_P^2 - Y_P^2}{2\ (\frac{4}{3} R)} \qquad (4.30)$$

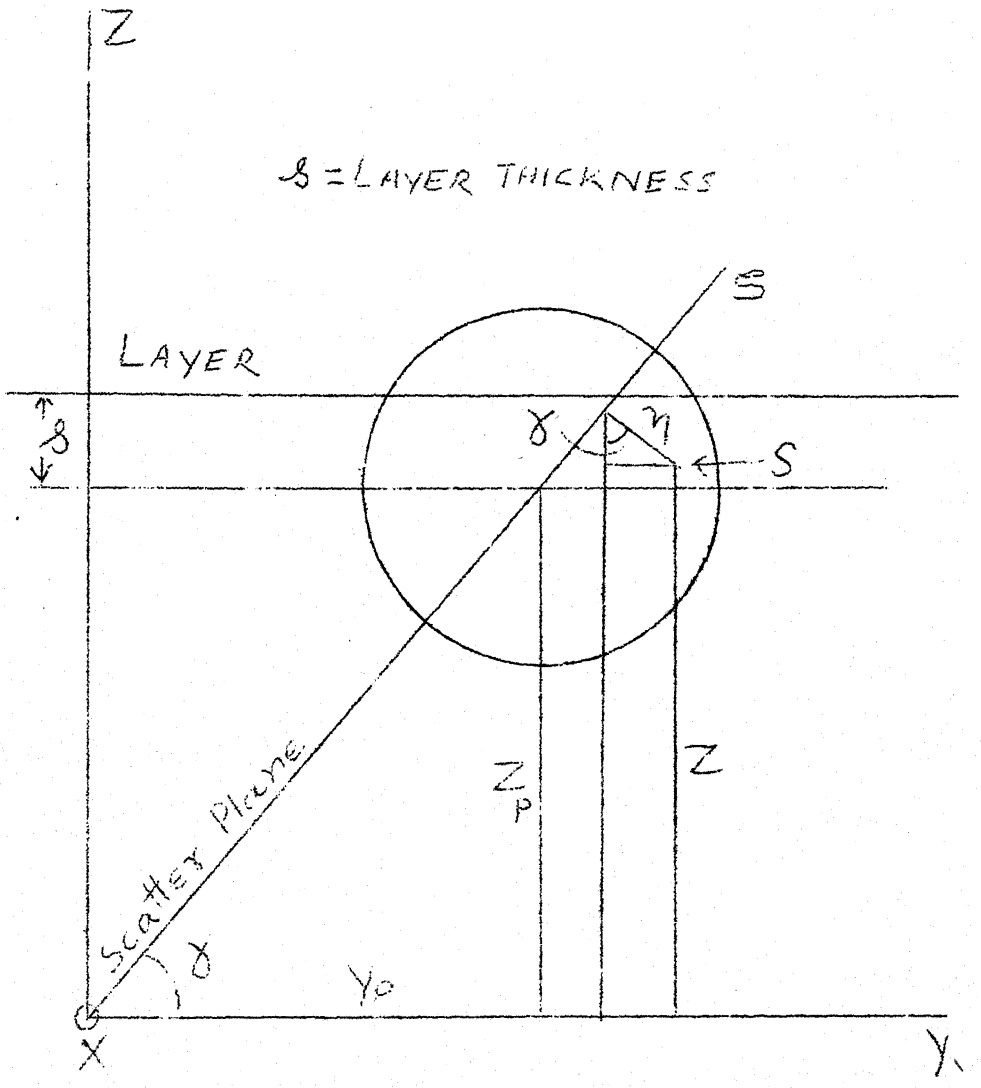

FIG 4.3 SCATTER ELEMENT HEIGHT ABOVE EARTH'S SURFACE

Thus knowing all the parameters, the value of the scatter integral is computed in order to determine the system response.

4.3 Polarization effects:

Consider Fig. 4.3A. The angle χ is between $\bar{L}_R$ and $\bar{E}$ and $\bar{E}$ is normal to $\bar{P}_T$. In case of horizontal polarization $\bar{E}$ has components in X and Y directions only. In case of vertical polarization $\bar{E}$ has components in all directions.

For horizontal polarization:

Only direction of $\bar{E}$ and $\bar{L}_R$ is of any significance. It is assumed that (Lammers, 1970)

$$\frac{E_X}{E_Y} = \frac{-Y}{D+X} \quad , \quad E_Z = o$$

then

$$\bar{E} = (-Y;\ D + X;\ o\ )$$

$$\bar{L}_R = (D - X;\ -Y;\ -Z)$$

$$\therefore \cos\chi = \frac{-Y \cdot 2D}{\left\{\left[(D+X)^2+Y^2\right]\left[(D-X)^2+Y^2+Z^2\right]\right\}^{1/2}} \qquad (4.31)$$

The factor for accounting for the polarization is determined from (4.31) as

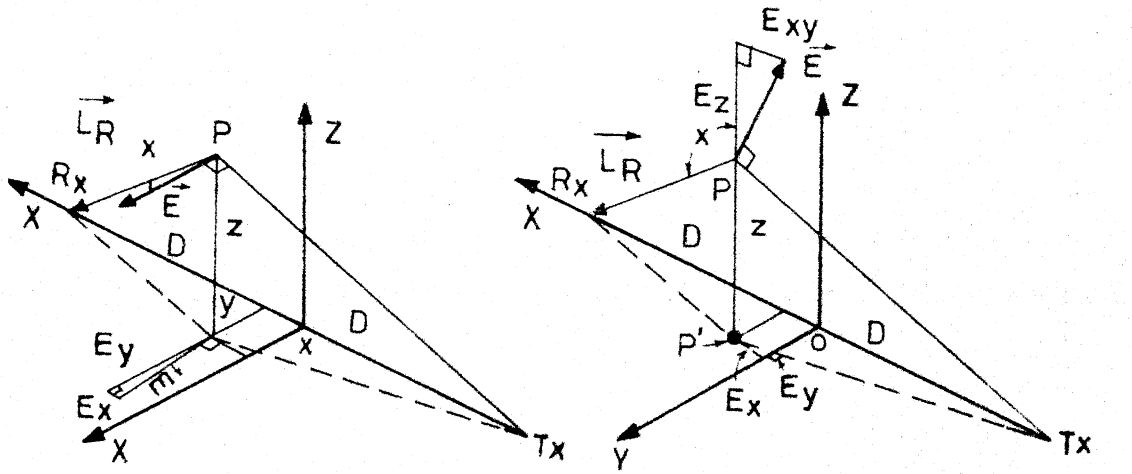

FIG. 4-3A. POLARIZATION EFFECT ON SCATTER SIGNAL

$$\sin^2\chi = 1 - \cos^2\chi$$

For vertical polarization:

The direction of $\bar{E}$ is such, in this case, that it is resolved into E_{XY} and E_Z. From treangle TP'P

$$E_Z = \left[(D + X)^2 + Y^2\right]^{1/2}$$

$$E_{XY} = Z$$

E_{XY} can be further separated into its constitutent components E_X, E_Y as

$$E_X = \frac{-(D + X)\, E_{XY}}{\left[(D + X)^2 + Y^2\right]^{1/2}}$$

and

$$E_Y = \frac{-Y \cdot E_{XY}}{\left[(D + X)^2 + Y^2\right]^{1/2}}$$

Multiplying each component with $\left[(D + \bar{X})^2 + Y^2\right]^{1/2}$ yields $\bar{E}$ as

$$\bar{E} = \left[-(D + X) \cdot Z;\ -Y \cdot Z;\ (D + X)^2 + Y^2\right]$$

$$\bar{L}_T = \left(-(D + X),\ Y, Z\right)$$

$$\therefore \cos\chi = \frac{-Z\,(D + X)\cdot 2D}{\left\{\left[Z^2(D+X)^2 + Y^2\right] + \left[(D+X)^2 + Y^2\right]\right\}^{1/2} \cdot \left[(D+X)^2 + Y^2 + Z^2\right]^{1/2}} \qquad (4.32)$$

The polarization factor is therefore

$$\sin^2\chi = 1 - \cos^2\chi$$

The angular range of polarization is

$$(\frac{\pi}{2} - \theta) \leq \chi \leq (\frac{\pi}{2} + \theta)$$

For Kanpur-Nainital Link, the value of θ for grazing incidence and fixed antenna position is 38.8 MR. However the beam swinging in the plane perpendicular to the great circle plane results in appreciable change in θ value. Therefore the term $\sin^2\chi$ is not neglected while computing the received power. Further the feed to the antenna dish is vertically polarized for this link. Therefore expression (4.32) is made use of for calculation of polarization factor.

4.4 Results of Simulation:

A system response is simulated taking into consideration the parameters of Kanpur-Nainital link. The simulation program is given at appendix 'A'. The single-layered model consists of the horizontal layer of 100 M vertical extent. This layer is assumed to be located at the center of the common volume. The beam swinging in the vertical plane is achieved by considering

the heights of layers at 2.0 Kms, 5.0 Km and 8.0 Kms. above the surface of the earth. For each layer height, the variations in the power received as a function of cross path variations are obtained by varying the value of Y. This provides system response for cross-path beam-swinging.

The simulation also accounts for system response for different layer dimensions. For this purpose a layer of 400 meters vertical extent is chosen at 5.0 Km height.

The condition of encountering more than one layer within the common volume is taken care of by chosing two layers of 100 meters width each separated by a distance of 500 meters. The layers are assumed to lie symmetrically on either side of the center of the common volume.

The power received for various layer heights considered for different Y-positions is plotted in Fig. 4.4. Fig. 4.5 depicts variations of the length of common volume ΔX as a function of scatter position. The values of scattering angle θ in mid path and great

circle plane are shown in Fig. 4.6. For a representative layer of 400 meters at a height of 5.0 Kms, the system response for different values of exponent $p = 2, \frac{11}{3}$ and 5 is shown in Fig. 4.7. The system response for two layers of 100 meters thickness, separated by 500 meters and situated symmetrically on either side of the center of the common volume, is plotted in Fig. 4.8. The height of the common volume center point is assumed to be 5 Km above the surface of the earth.

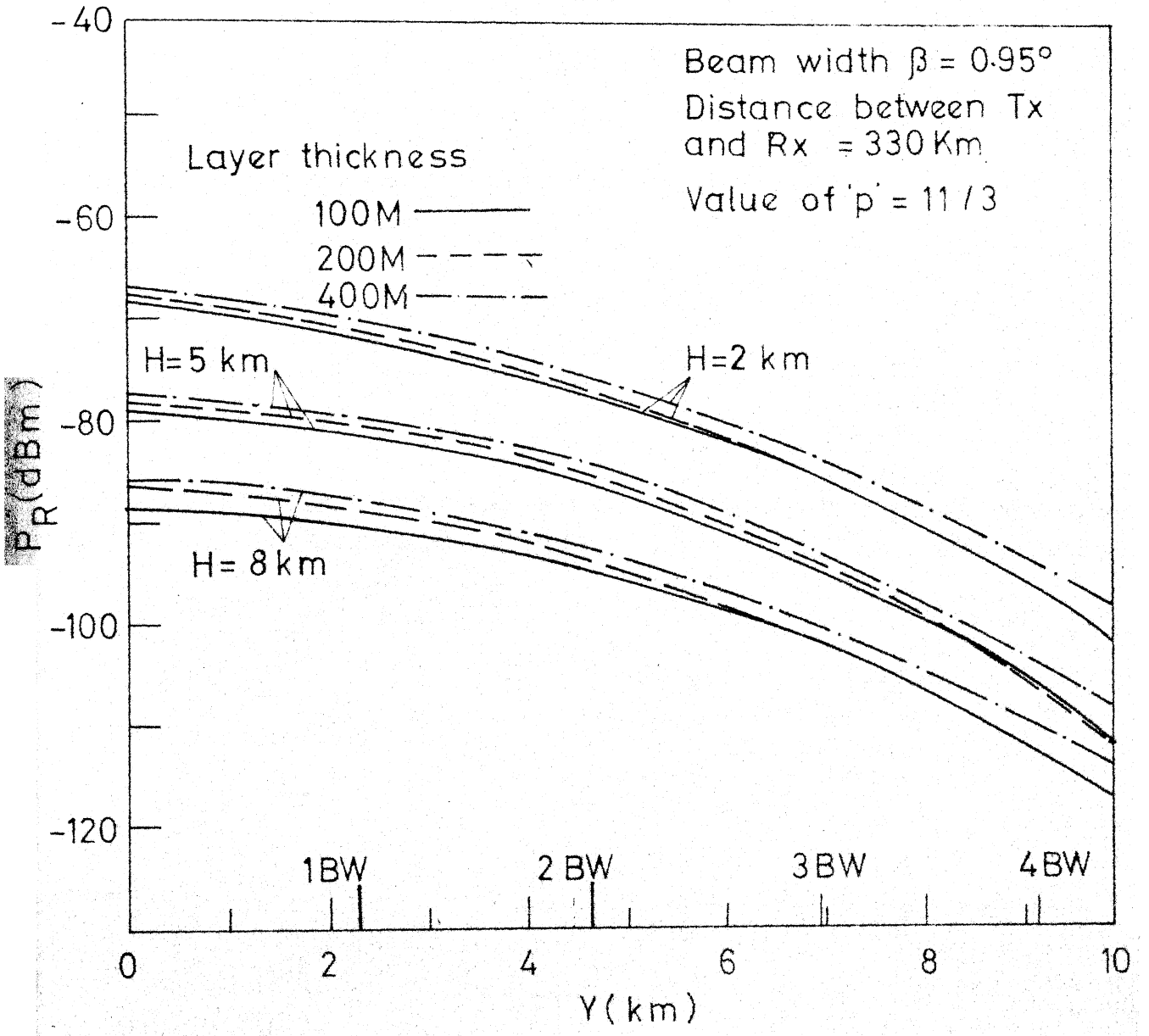

FIG. 4.4 SYSTEM RESPONSE FOR DIFFERENT LAYER THICKN
AT DIFFERENT HEIGHTS.

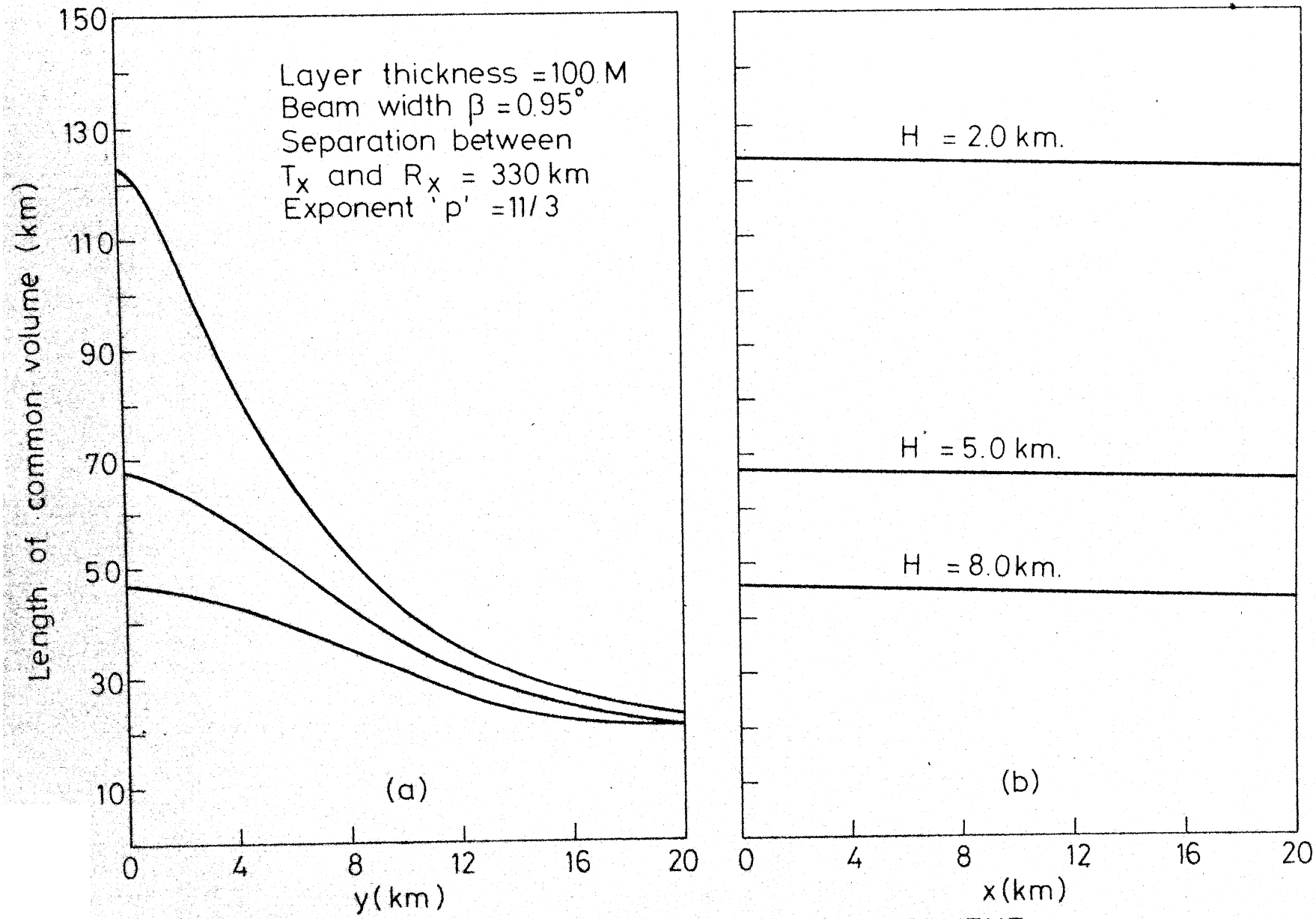

FIG.4.5 LENGTH OF COMMON VOLUME VS. DISPLACEMENT.

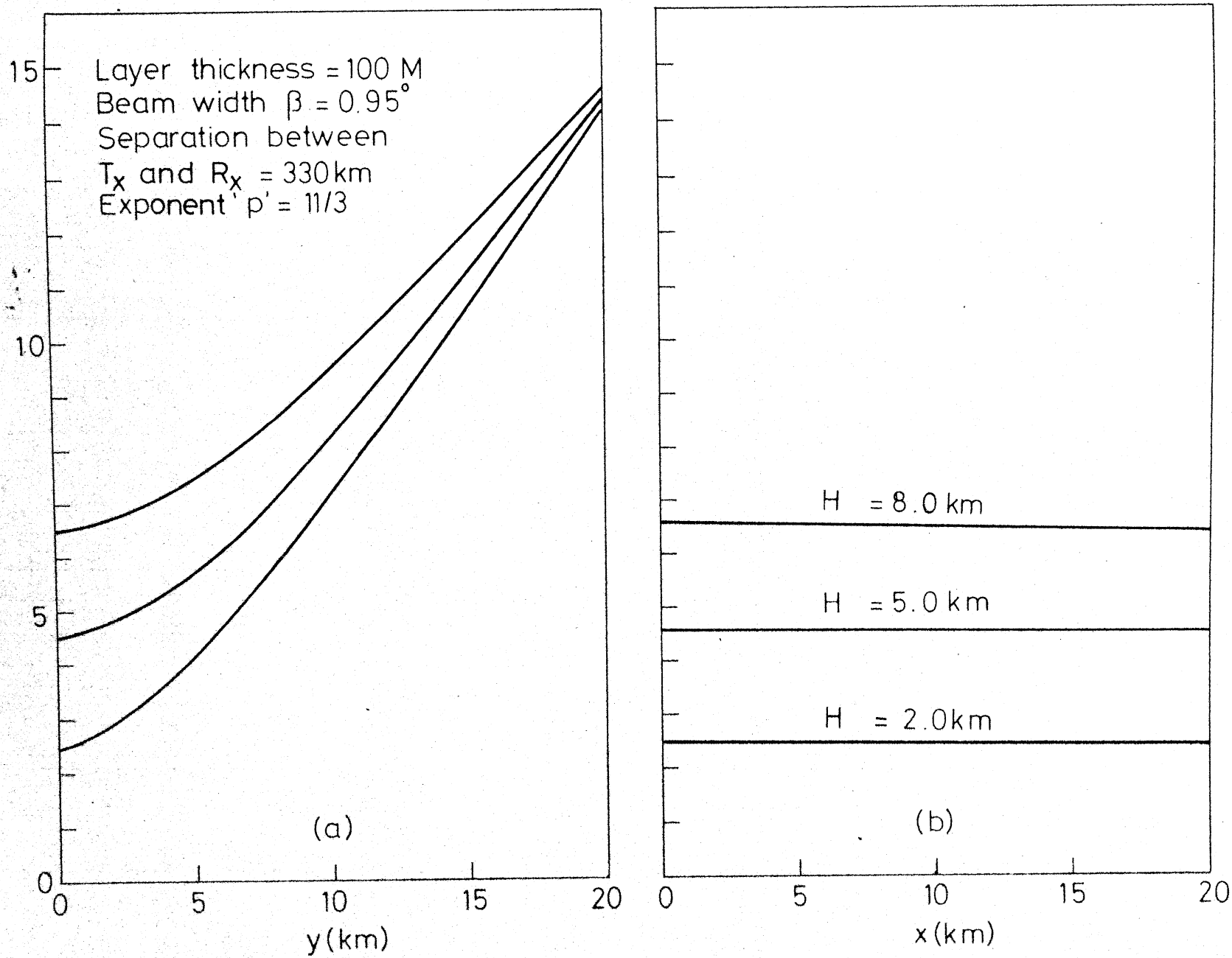

FIG 4.6 SCATTERING ANGLE FOR DIFFERENT SPATIAL POSITIONS.

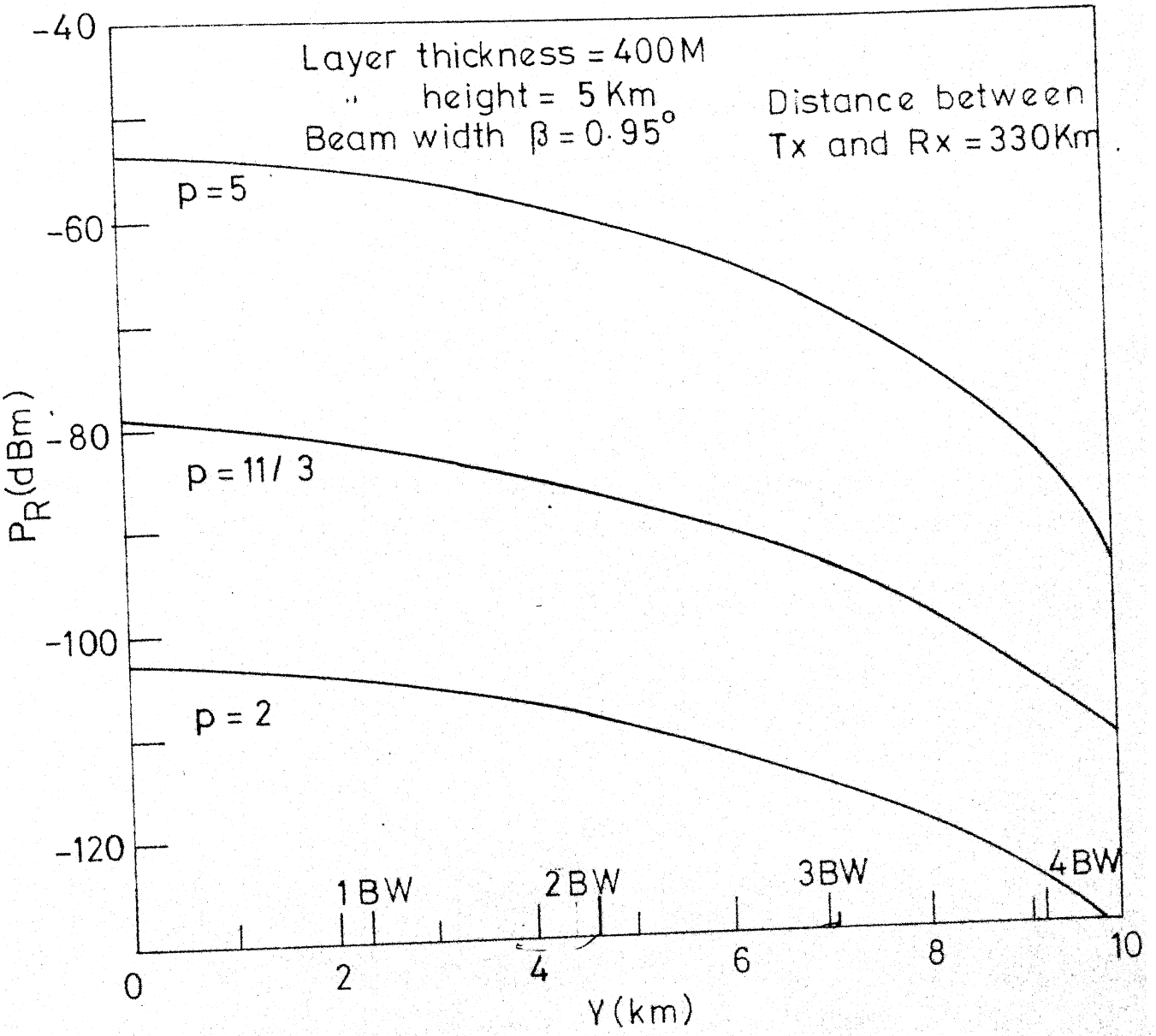

FIG. 4.7 SYSTEM RESPONSE FOR DIFFERENT VALUES OF EXPONENT 'p'

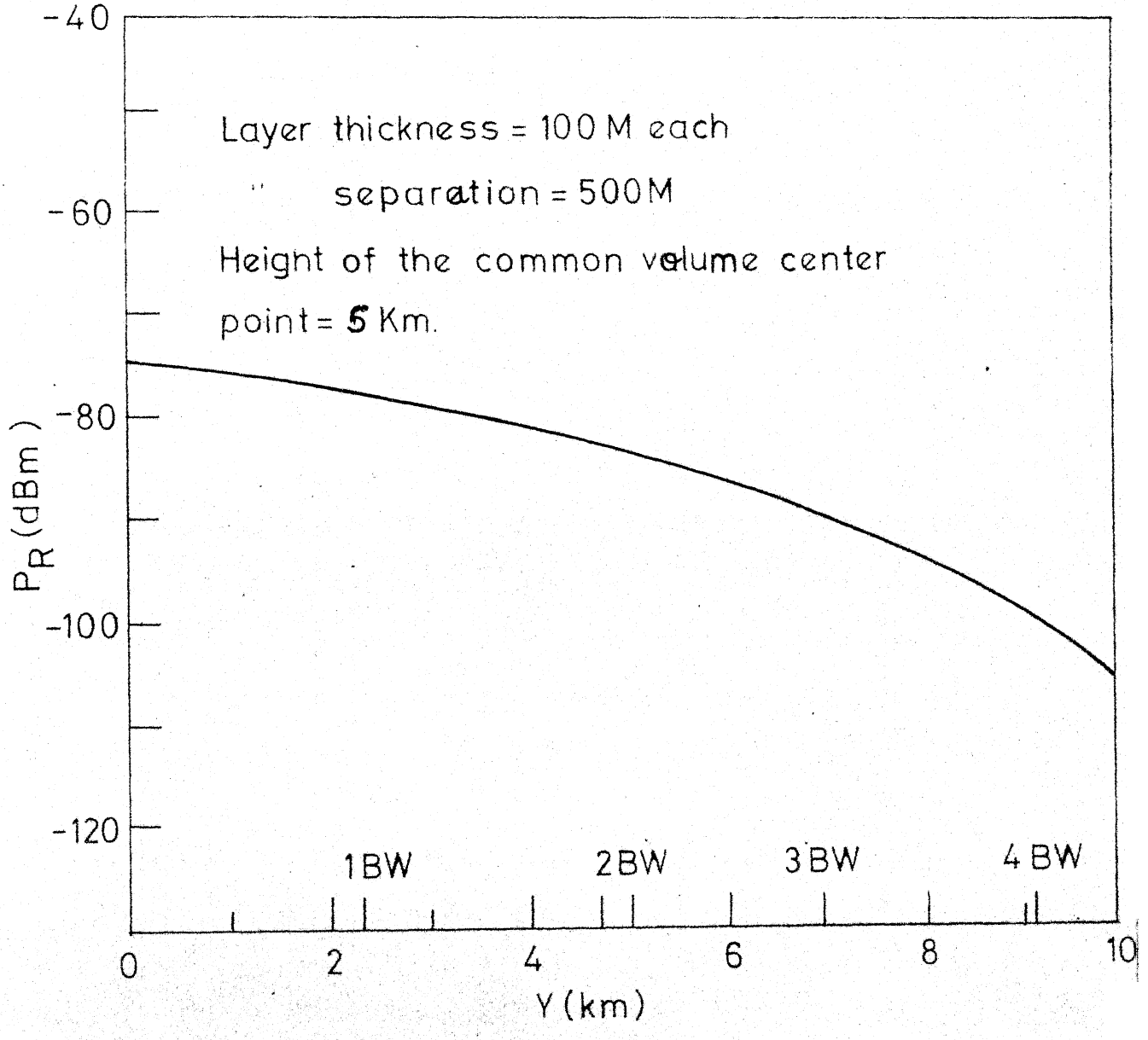

FIG. 4.8 SYSTEM RESPONSE FOR MULTI LAYERS

CHAPTER V

SPECULAR-REFLECTION CONTRIBUTION TO RECEIVED POWER

5.1 Review of Friis Theory of reflection from infinite flat layer:

In terms of this theory (Friis et.al; 1957) uncorrelated reflections from the assumed layers in atmosphere caused by relatively sharp gradients of refractive index are assumed to be responsible for propagation of signal beyond radio horizon. This may not be true entirely, in that, it has been established that the scattering of radio waves from turbulent changes in the refractive-gradients takes place accompanied by the specular reflection from heights where mean vertical refractive gradients show a sudden change (Atlas et.al; 1969). But the specular reflection, which by its very nature takes place only near the great circle, is some times found out to be several times the magnitude of the power received via scatterers. Hence the necessity of determining the specular contribution.

The reflections from any layer depends on the amplitude reflection coefficient 'q', a function of incidence angle and layer dimensions with respect to Fresnel-zone dimensions. There would be three different cases based on the size of layer considered (Fig. 5.1).

Case I

Large layers:

In this case the layer is assumed to be a plane, perfectly reflecting surface of unlimited extent, which is also the basic assumptions made for scatters (infinitely long layer with very narrow vertical extent). The power received in this case is given as

$$P_R = P_T \cdot \frac{A_T \cdot A_R}{4\lambda^2 (D)^2} \cdot q^2 \qquad (5.1)$$

where 'q' is called the co-efficient of reflections and A_T , A_R are effective areas of transmitting and receiving antennas. The expression (5.1) is applicable only if

(a) Horizontal extent of layer is much greater than $\sqrt{2D\lambda}/\varphi$, φ being the incident/reflection angle for the signal, and

(b) width of the layer is greater than $\sqrt{2D\lambda}$, 2D being separation of transmitter and receiver.

Case II

Small layers:

This is the case when the layer dimensions are very small when compared to the Fresnal zone dimensions, but are fairly large as compared to the wave length. In that case (Friis, 1957)

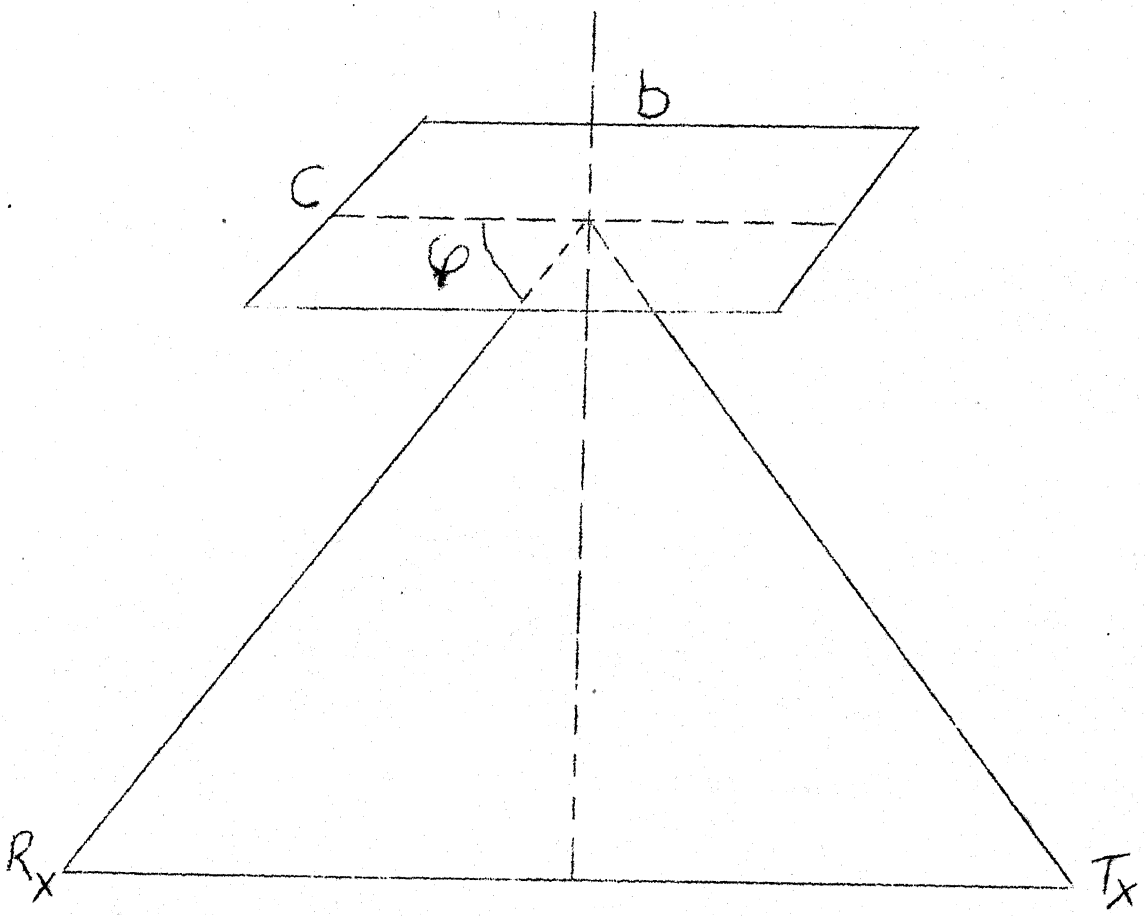

FIG 5.1 REFLECTION FROM FLAT LAYERS

$$P_R = P_T \cdot \frac{A_T \cdot A_R}{\lambda^4 (D)^4} \cdot C^2 \, (b\varphi)^2 \cdot q^2 \qquad (5.2)$$

where C is width of layer & b is length of layer.

Case III

Layers of Intermediate size:

In this case C is large but $(b.\varphi)$ is assumed bc fairly small as compared to the Fresnel-zone dimensions; so

$$P_R = P_T \cdot \frac{A_T \cdot A_R}{2\lambda^3 (D)^3} \cdot (b.\varphi)^2 \cdot q^2 \qquad (5.3)$$

Now many of the layers contributing to the power received are not neccssarily in the horizontal plane. They may be oriented in any direction. The reflection, therefore would take place from layers located on "off" as well as 'ON' side of great circle path. If V is the common volume and there are N contributing layers per unit common volume, then for intermediate layer size

$$P_R = P_T \cdot \frac{A_T \cdot A_R}{2\lambda^3 (D)^3} \int_V N.\varphi^2 \cdot q^2 \cdot dV \qquad (5.4)$$

The only assumption made in this case is that the number of layers per unit volume does not alter throughout the common volume. If N' is taken as change of refractivity

gradient (or the change in the gradient of dielectric constant at the boundary layers), then

$$q = \frac{N' \cdot \lambda}{16\pi\varphi^3} \qquad (5.5)$$

The specular reflectivity η_s has been used in formal analog with $\sigma(\theta)$, the turbulent reflectivity for calculation of specular reflection power contribution. By its very definition, η_s will have finite value only at the position X = 0, Y = 0, Z = some finite values, lying within the common volume. Off-setting the antenna beams off the midpath position, the power actually received through reflection is reduced by the antenna gain product along the great circle path.

The effective areas of the antennas are related to the respective gain functions by

$$A = \frac{G\lambda^2}{4\pi}$$

Substituting for A_T and A_R, expression (5.1), the received power due to reflection from infinitely large, flat layer becomes

$$P_R = P_T \frac{\lambda^2 \cdot G_R\, G_T}{(4\pi)^2 \cdot (2D)^2} \cdot q^2 \qquad (5.6)$$

5.2 Calculation of reflected power:

The significant contribution to the power received

due to specular reflection is due to reflection from the great circle path (Lammers, 1970). If height of the reflection point from the surface of the earth is H*, then the reflection point will be described by the coordinates

$$X = 0,\ Y = 0,\ Z = H_o + H^*$$

and the center of the common volume

$$X_P\ ,\ Y_P,\ Z_P = H_o + H - \frac{X_P^2+Y_P^2}{2(\frac{4}{3} R)} \qquad (5.7)$$

Consider. Fig. 5.2 showing reflection point as P*, P being the center of common volume.

The distance of reflection point from transmitter and receiver locations is

$$L = \left[(D)^2 + (H_o + H^*)^2\right]^{1/2} \qquad (5.8)$$

Considering Fig. 4.1 and substituting the values of expression (5.7) gives

$$S^2 = Y_P^2 + Z_P^2 = Y_P^2 + \left[H_o + H - \frac{X_P^2+Y_P^2}{2(\frac{4}{3} R)}\right]^2 \qquad (5.9)$$

Substituting expression (5.9) in the expressions (3.4) and (3.7) gives the distance of center of common volume from transmitter and receiver as

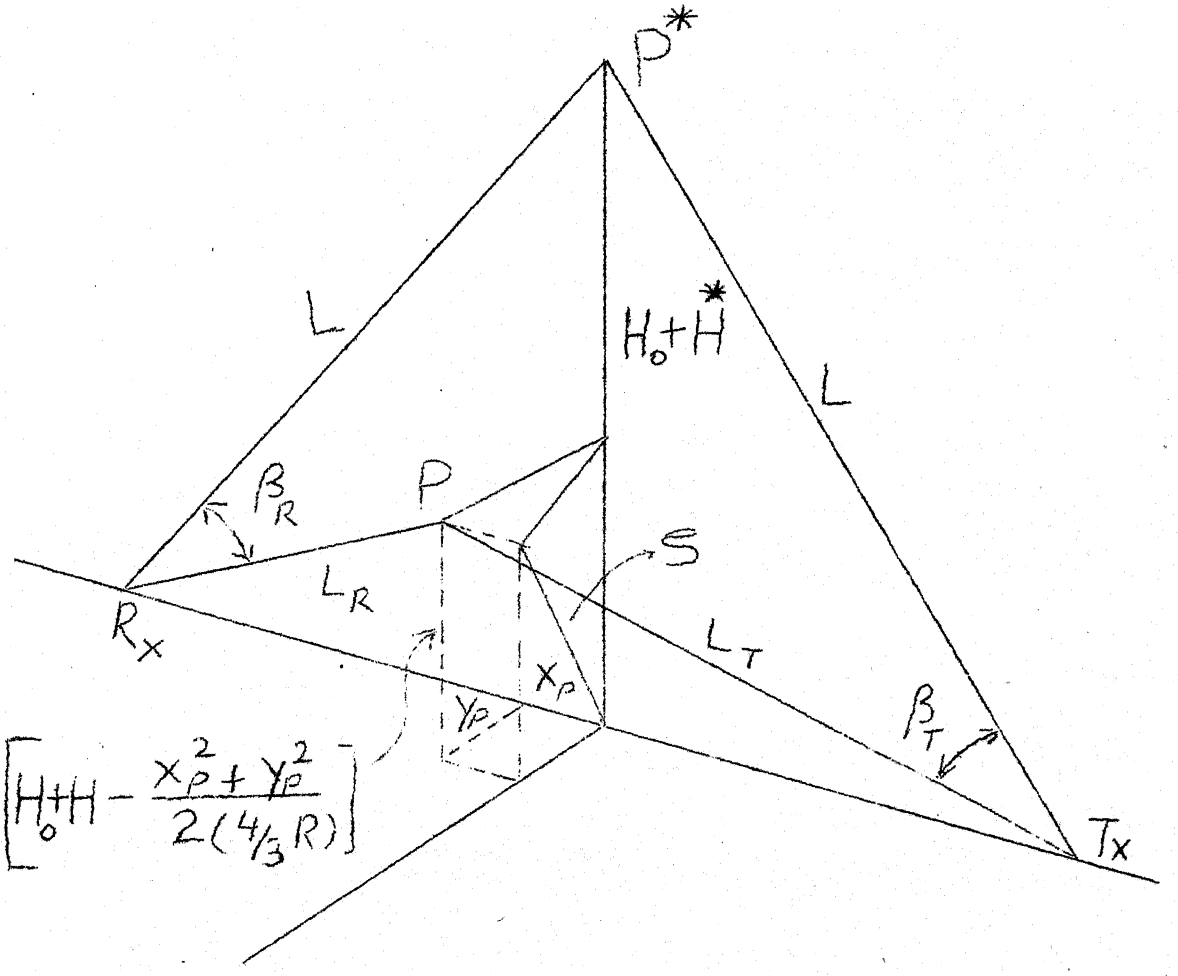

FIG 5.2 SPECULAR CONTRIBUTION

$$L_T = \left[(D + X_P)^2 + Y_P^2 + (H_o + H - \frac{X_P^2 + Y_P^2}{2(\frac{4}{3} R)})^2 \right]^{1/2} \qquad (5.10)$$

$$L_R = \left[(D - X_P)^2 + Y_P^2 + (H_o + H - \frac{X_P^2 + Y_P^2}{2(\frac{4}{3} R)})^2 \right]^{1/2} \qquad (5.11)$$

Then from Fig. 5.2

$$\overline{PP^*} = \left[X_P^2 + Y_P^2 + (H^* - H + \frac{X_P^2 + Y_P^2}{2(\frac{4}{3} R)})^2 \right]^{1/2} \qquad (5.12)$$

and so

$$\cos\beta_T = \frac{L^2 + L_T^2 - \overline{PP^*}}{2 L \cdot L_T} \qquad (5.13)$$

and $$\cos\beta_R = \frac{L^2 + L_T^2 - \overline{PP^*}}{2L \cdot L_T} \qquad (5.14)$$

Expressions (5.13) and (5.14) give the values of β_T and β_R, which, substituting in expression (3.18) yield the antenna gain functions product $G_T G_R$. This antennas - gain product when substituted in basic received power scatter-integral (4.24) gives out the power received due to the specular reflection.

CHAPTER VI

DISCUSSION AND CONCLUSION

6.1 Discussion on results obtained:

The model simulated to obtain the system response consists of assumed layer widths typically less than the vertical extent of the common volume. The received power is calculated with respect to three different layer heights 2,5 and 8 Kms above the surface of the earth. The layer height conicides with the centre of the common volume. Besides these, the received signal for the grazing incidence, which is the condition of the actual Kanpur-Nainital link, and height 1.6 Km above the surface of the earth (common volume at 3.2 Km above the x-y plane) is also computed.

The discussion on the results obtained can be broadly devided into three categories, namely, (a) changes in scattering angle for different common volume positions in space (b) changes in linear extent of common volume vs the position in space and (c) effect of beam swinging on the received power. These are discussed separately.

Change in Scattering angle θ:

The beam swinging along the great circle path, keeping cross path position and height of common volume above the surface of the earth unaltered, has very little effect on the scattering angle. For beam swinging upto 20 Kms the change in the scattering angle, is of the order of 0.1 degree only. This is shown in Fig 4.6. However with variations in cross path position θ changes considerably. Upto a change in Y of about 2.0 Km, the change in θ is very small. However beyond this point any further increase in Y increases θ in an asymtotic manner. At distance of about 20 Km, the θ values for the three different layer heights chosen for simulation tend to converge to the same point. The change in θ for different heights is

For layer height 2 Km 2.5° to 14.4°

For layer height 5 Km 4.6° to 14.6°

For layer height 8 Km 6.6° to 14.7°

The increase in θ reduces the power received by the factor $\left(\sin \frac{\theta}{2} \right)^{-p}$. Thus the expected drop in signal level is very small for Y = 2 Km and pronounced beyond this value.

Changes in common volume length:

The length of common volume is maximum at the grazing incidence of the antenna beams in the mid path plane. Any swing of the beams along and/or across the path reduces it. However for a given Y position and given layer height, this change is very small for along path variations than that for cross path variations (Fig. 4.5). The common volume decreases with height. But the change in the length of common volume with reference to its spatial position is more for lower layer heights than that for higher heights. It is seen that for the three layer heights chosen for the simulation model the change in length of common volume is very small upto about Y=2 Km. Further beyond about Y=18 Kms the length of common volume (and hence common volume) is approximately same for all the height levels considered. Thus beyond this point the reduction in the received signal level if any, would not be due to the common volume reduction but entirely due to changes in scattering angle and such allied factors of the scatter integral.

The length of the common volume is derived from eqn. (3.6) which is not dependent on scatter plane inclination γ . It can be said, therefore, that the common volume centre cross-section is approximately independent of the scatter position within the region considered for simulation purposes.

Received power versus the spatial position:

The signal level drops with height and position across the signal path (Fig. 4.4 and 4.7). The apparent width of the layer increases along path and decreases across path.

For a representative layer of width 400 meters and located at a height of about 5.0 Km for exponent $p = 2, \frac{11}{2}, 5$ the variations in received power with Y is shown in Fig. 4.7. The plot reveals that the received signal has approximately the same statistical properties for $p = 2$ and $\frac{11}{3}$. In case of p=5, the plot shows approximately same statistical properties upto 8 Kms beam swinging. However beyond this point, the fall in the received power level is slightly more.

The value of P_R for $p = \frac{11}{3}$ is more close to the observed values from the experimental Kanpur - Nainital link.

The system response for different layers thickness is shown in Fig. 4.4. Three layers of 100, 200 and 400 meters each are considered and signal received computed. It is seen that for the layer widths 100 meter and 200 meters, the signal level is approximately same for respective heights considered. However when the layer thickness is increased to 400 meters, at lower height (2 Km), the signal level is more by about 1.5 db in the midpath plane and drops down to the 100 meter level beyond Y = 7 Kms. This indicates that the layer width of 100 meters or so is in a way representative of the actual tropospheric common volume.

The simulated signal level in the mid path plane for the grazing incidence is -66.9 dBm . The observed maximum signal level for our link is approximately -63 dBm. Thus there is disparity of about 4 dBm. This appears to be due to the fact that the contribution due to specular reflection is not included in the simulated model. Further in the actual experimental

set up large extent of the signal path lies along one of the major river. In such a case, the lapse rate of moisture with height is expected to be very high. This will create favourable conditions for ducting. Thus the observed signal is likely to have a component due to specular reflection and a component due to ducting. This appears to explain the fact that the signal strength obtained from simulation is less than the observed value.

6.2 Conclusion:

In this thesis attempts have been made to determine the effects of the system geometry and the layered atmospheric sturcture of the troposphere on the received signal. The simulated results indicate lower signal strength than the experimental results. One of the troposphere parameters function C_n^2 has been used with value equal to $5. \times 10^{-12}$ throughout the simulation. But this enters linearly into the received signal. Therefore any change in the signal level by about few dBm will yield any value of C_n^2 signal distribution.

For the simulation purposes, the medium is assumed to be isotropic at the frequency and scattering angle used. The shadow-zone of the earth increases monotomically in height at greater distance across path. Hence extended coverage of upto 20 Kms beam swinging used for simulation may not give accurate results on the actual link.

6.3 Recommendations:

The simulation model developed in this thesis does not indude specular reflection contributions. The mathematical treatment given in chapter V gives analytical expression for this contribution.

Also the scattering layers are assumed to be horizontal. The effect of the presence of the tilted layers within the common volume has not been considered. The atmosphere has been assumed to be isotropic for the wavelength and scattering angle used, which may not be true in actual case.

Hence the simulated model could be further extended to take care of

a) Anisotropy of the medium
b) Contribution due to specular reflection and
c) Effect of presence of one or more tilted layers within the common volume.

BIBLIO-GRAPHY

1. Atlas, D. (1969), 'Measurement of cross wind by non coherent dual arm bistatic radio troposcatter technique', Tech. Rep. 10, Laboratory for Atmospheric Probing, University of Chicago - Illinois.

2. Atlas, D.; Srivastava, R.C.; Carbone, R.E.; Sargent, D.E. (1969), 'Doppler cross wind relations in radio troposcatter beam swinging for a thin layer', Tech. Rep. 8, Laboratory for Atmospheric Probing, University of Chicago, Illinois.

3. Birkemeir, W.P.; Thomson, D.W.; Merrill Jr., H.S.; Beamer, G.M.; Bergmann, G.T. (1968) 'Observation of wind produced doppler shifts in tropospheric scatter propagation', Rad. Sc. 3(4) pp. 309-317.

4. Bassi, R.K. (1974), 'A study of troposcatter signal characteristics based on the random layered scatter model', M.Tech. thesis, Dept. of Elec. Engg. I.I.T. Kanpur.

5. Booker, H.G., and Gordon, W.E. (1950), 'A theory of radio scattering in troposphere', Proc. IRE vol. 38, pp. 401-412.

6. Bures, K.J. (1975), 'High resolution imaging of tropospheric radio scatters', IEEE Trans. on Aerospace and electronic systems, AES-11, No. 2, pp. 137-146.

7. Dalukhanov, M. (1971), 'Propagation of radio waves', Mir Publishers, Moscow.

8. Eklund, F. and Wickerts, S. (1968), 'Wave length dependence of the microwave propagation for beyond radio horizon', Rad. Sc. 3(11), pp. 1066-1074.

9. Friis, H.T.;Crawford, A.B.; and Hog, D.C. (1957), 'A reflection theory for reflection for propagation beyond the horizon', BSTJ Vol36,pp. 627-644.

10. Fengler, C. (1971), 'Remote sensing and Atmospheric layers, AGARD Symposium, Colorado Spuner, USA, June 21-25.

11. Gjessing, D.T. (1962), 'Determination of permittivity variations in the troposphere by scatter propagation gation methods, Proc. IEEE London (109). pp. 447-455, (IEEE Mon graph No. 510E).

12. Gjessing, D.T. (1964), 'An experimental study of variation of tropospheric scattering cross-section and air velocity with position in space', IEEE Trans., Antenna & Propagation, AP 12(1), pp. 65-73.

13. Gjessing, D.T. (1969), 'Atmospheric structure deduced from forward scatter wave propagation experiments', Rad. Sc. 4(12); pp. 1195.

14. Gupta, G.C. (1973), 'Tropospheric probing by scatter communication', M.Tech. thesis, Dept. of Elec. Engg., I.I.T. Kanpur.

15. Lammers, U.H.W., Short Jr., J.A. (1970), 'Investigation of layered tropospheric structures using forward scatter techniques', Environmental research papers No. 311, AFCRL-70-0073, Airforce Cambridge Research Laboratories, Bedford.

16. Lammers, U.H.W. (1973), 'Imaging properties of monostatic and bistatic radars', Rad. Sci., vol. 8, Number 2, pp. 89-101.

17. Lammers, U.H.W. and Day, J.W.B. (1972), 'Comparison of turbulent layer models and high resolution forward scatter results', pp. 27-1, 27-10.

18. Mathur , N.C. ;Mehra, D.K. and Raman, A. (1974), 'Atmospheric refractive Studies with airborne microwave refractometer', Tech. Report No. TR-22-74, ACES, I.I.T. Kanpur.

19. Mitra, A.P., Reddy, B.M. and Santosh Aggarwal(1975), 'Tropospheric propagation and Antenna measurements', Collection of lecture notes of first advance course, Radio Science Division, NPL, pp. 140-154.

20. Ottersten, Hans (1969), 'Atmospheric structure and radar back scattering in clear air', Rad. Sc. 4(12), pp. 1179-1192.

21. Silverman, R.A., (1957), 'Turbulent mixing theory applied to radio scattering', J. Applied Physics, vol. 27, pp. 699.

22. Staras, H. and Wheelon , A.D. (1959), 'Research on tropospheric propagation in U,S.', Trans. IRE , vol. AP-7, No. 1, pp. 80.

23. Tatarski, V.I. (1961), 'Wave propagation in a turbulent medium, McGraw Hill Book Company Inc. 1961.

24. Wheelon, A.D. (1972), 'Back scattering by turbulent irregularities', Proc. IEE 60, pp. 252.

25. Mathur, N.C. and Mehra, D.K. (1976), 'Doppler Cross-wind relations for Kanpur-Nainital Troposcatter link', JIETE, Aug. 76.

26. Majumdar, S.C.(1974), 'Transhorizon tropospheric propagation studies over the Indian subcontinent', Report No. 13, Centre of Research on Troposphere, N.P.L., New Delhi.

27. Chisholm, J.H.(1956), 'Progress of tropospheric propagation research related to communication beyond the horizon', Trans IRE CS-4, No. 1, pp. 6.

28. Rama Rao, C.T.(1975)'Computer simulation of scattering functions for Kanpur-Nainital rake troposcatter system', M.Tech. Thesis, Deptt. of Elect. Engg., I.I.T. Kanpur

29. Birkmeier, W.P.; Fontaine, A.B.; Gage, K.S.; Jasperson, W.A. (1974), 'A comparison of rake measured scattering layer signatures with radio-sonde data', RADC-74-17, Rome Air Development Center, Final Tech. Rep.

APPENDIX 'A'

```
/ JOB
/ FOR MAIN
IOCS(CARD,TYPEWRITER)
ONE WORD INTEGERS
NON PROCESS PROGRAM
*************************************************************************

     SIMULATION PROGRAM FOR CALCULATION OF THE POWER RECIEVED FROM THE
     TROPOSPHERE CONSIDERING TROPOSPHERETO BE LAYERED STRUCTURE.


     THE SIMULATICN PROGRAM HAS BEEN RUN ON IBM 1800 COMPUTER.
     THE BASIC ASSUMPTIONS MADE FOR THE PURPCSES OF ANALYSIS ARE
               1)THE EARTH IS ASSUMED TO BE A SPHERE OF  RADIUS 4/3 TIMES
                 THE ACTUAL RADIUS TO TAKE CARE OF THE DECREASE IN THE
                 VALUE OF REFRACTIVITY WITH INCREASE IN HEIGHT.
               2)THE RECIEVER AND TRANSMITTER ANTENNAS ARE ASSUMED TO BE
                 LOCATED ON THE SURFACE OF THE EARTH.


*************************************************************************

     FOLLOWING ARE THE INPUT PARAMETERS ----------------------------------

     2D=THE SEPARATION BETWEEN THE TERMINAL STATIONS.
     R=EFFECTIVE RADIUS OF THE EARTH WHICH IS TAKEN AS 8500 KMS.
     PT=TRANSMITTED POWER IN WATTS.
     ALAMD = THE SYSTEM WAVELENGTH BEING USED
     BEETA=HALF BEAM-WIDTH OF THE ANTENNA BEAM WHICH IS .950 DEGREES.
     HT=THE HEIGHT OF THE SCATTERING LAYER. THREE DIFFERENT HEIGHTS
     NAMELY 2,5, AND 8 KM ARE CONSIDERED FOR THE PURPOSES OF THE SIMULATI

*************************************************************************


     PROGRAM STARTS
     REAL NT,NR,LT,LR,NTMAX,NRMAX,NETMX,NETMN,NEETA
     INTEGER TN
     DIMENSION PRWAT(50), PRDBS(50)
     DIMENSION  H1(10),H2(10)
     COMMON//XP,ZETAP ,NEETA,ZTLOW ,THETA ,FO
     TN=1
     ALAMD=.14826
     PT=1000.
```

```
      R=8.5E 06
      D=165.E 03

      PAI IS THE CONVERSION FACTOR FOR CONVERTING RADIANS TO DEGREES
      PI=4.*ATAN(1.)
      PAI=PI/180.
      DELX=4.E 03
      DELY=500.
      BEETA IS THE HALF BEAM-WIDTH OF THE ANTENNA BEAM.
      BEETA=PAI*.95/2.

      CN IS THE STRUCTURE FUNCTION  COEFFICIENT.
      CN=5.E-12
      DELZ=100.0
      HT=2.E 03
      HO=0.5*D*D/R
      READ(5,127) FO
 27   FORMAT(F6.5)

      NOL DEFINES THE NUMBER OF THE LAYERS BEING CONSIDERED

      NOL=1
      DO 31 NN=1,NOL
      ATKNS IS THE THICKNESS OF THE LAYER BEING CONSIDERED
      ALOBD IS THE LOWER BOUNDARY OF THE LAYER
       READ( 5,32)  ATKNS
      ALOBD=HT+HO
       H1(NN)=ALOBD
       H2(NN)=H1(NN)+ATKNS
 31       CONTINUE
 32   FORMAT(2X,E15.8)

      XP,YPAND ZP DEFINE THE ARBITRARY CENTER OF THE COMMON VOLUME

  8   XP=0.0
  9   YP=0.0
      J=1
      ZP=HPRIM+HT

      HPRIM IS THE DISTANCE OF THE EARTH'S SURFACE FROM THE X-Y PLANE FOR

  5   HPRIM=HO-0.5*(XP*XP+YP*YP)/R

      X,Y AND Z DEFINE ANY ARBITRARY POINT. HERE THIS POINT IS ASSUMED TO
      COINCIDE WITH THE CENTER OF THE COMMON VOLUME P

      X=XP
      Y=YP
```

```
      Z=ZP
      DEN=SQRT(YP*YP+ZP*ZP)
C
C     PRWAT(J) IS THE RECIEVED POWER IN MILLIWATS
C     FUNC IS THE VALUE OF THE INTEGRAND IN THE SCATTER INTEGRAL
C
      PRWAT(J)=0.0
      FUNC=0.0
       WRITE(TN,112) J,X,Y,HPRIM
  112 FORMAT(2X,3HJ= , I3  ,2X,6HX     =,E15.8,2X,6HY     =,E15.8,
     12X,6HHPRIM=,E15.8/2X,3H***, 5X,6H******,17X,6H******,17X,6H******)
       WRITE(TN,113)
113   FORMAT(8X,'THETA IN',11X,'GAMA IN',12X,'PR IN',11X,'PR IN'/8X,
     I  'DEGREES',12X,'DEGREES',12X,'WATTS',12X,'DBM'/)
      DO 200 K=1,40
      IF(YP) 22,22,23
 22   GAMA=89.475*PAI
      GO TO 24
 23   GAMA=ATAN(ZP/YP)-BEETA
 24   CONTINUE
      GAMA=GAMA+PAI*FLOAT(K)/40.
       GMADG=GAMA/PAI
      ZETAP=YP*COS(GAMA)+ZP*SIN(GAMA)
C
C     THETR AND THETT ARE THE AGLES MADE BY THE BORESIGHTS OF  THE
C     RECIEVER AND TRANSMITTER ANTENNA RESPECTIVELY.
C
      THETT=ATAN(ZETAP/(D+XP))
      THETR=ATAN(ZETAP/(D-XP))
C
C     THETA IS THE SCATTERING ANGLE.
C
      THETA=(THETT+THETR)/PAI
C
C     THIS PROGRAM  CALCULATES THE SLOPES OF THE  ANTENNA CONE TANGANT
C     PLANES AND HENCE THE X AND ZEETA LIMITS OF THE ONTEGRATION.
C
      TR1=SIN(THETR+BEETA)/COS(THETR+BEETA)
      TR2=SIN(THETR-BEETA)/COS(THETR-BEETA)
      TT1=SIN(THETT+BEETA)/COS(THETT+BEETA)
      TT2=SIN(THETT-BEETA)/COS(THETT-BEETA)
C
C
      XMIN= D*(TR2-TT1)/(TR2+TT1)
      XMAX=   D*(TR1-TT2)/(TR1+TT2)
      ZTMIN= 2.*D*TR2*TT2/(TR2+TT2)
      ZTMAX= 2.*D*TR1*TT1/(TR1+TT1)
C
```

```
C       THIS PROGRAM ENSURES THAT THE INTEGRATION STARTS ONLY WHEN THE
C       SCATTER PLANE COMES WITHIN THE ANTENNA CONES COMMON ZONE.
C
        IF(YP) 26,26,27
 26     EXPR=ZTMAX*COS(GAMA)-ZP*SIN(BEETA)/COS(BEETA)
        GO TO 28
 27     EXPR=ZTMAX*COS(GAMA)-(YP+(ZTMAX-ZTMIN)/2.)
 28     IF(EXPR) 7,200,200
  7     CONTINUE
C
C       ALNTH IS THE LENGTH OF THE COMMON VOLUME
C
        ALNTH=XMAX-XMIN
        ZEETA=Y*COS(GAMA)+Z*SIN(GAMA)
C
C       THIS PROGRAM CALCULATES THE VALUE OF THE POLARIZATION FACTOR
C       FOR KANPUR NAINITAL LINK THE ANTENNA HORN FEEDS ARE VERTICALLY
C       POLARIZED. HENCE THE EXPRESSION CALCULATED FOR ACCOUNTING OF
C       POLARIZATION EFFECTS IS FOR VERTICAL POLARIZATION .
C
        AK1=Z*Z*((D+X)**2+Y*Y)
        AK2=((D+X)**2+Y*Y)**2
        AK3=(D-X)**2+Y*Y+Z*Z
        AK=4.*Z*Z*D*D*(D+X)**2
        SKSQ=1.-AK/((AK1+AK2)*AK3)
C
C       LT AND LR ARE THE SQUARED DISTANCES OF POINT P FROM TX AND RX.
C
        LT=(D+X)**2+ZEETA*ZEETA
        LR=(D-X)*(D-X)+ZEETA*ZEETA
C
C       THIS PROGRAM DETERMINES THE NEETA LIMITS OF THE INTEGRATION
C       THE NEETA LIMITS ARE CALCULATED FOR THE VALUES OF NEETA GREATER
C
        NT=BEETA*BEETA-(ATAN(ZEETA/(D+X))-THETT)**2
        IF(NT-0.0) 200,200,1
    1   NTMAX=SQRT(NT*LT)
        NR=BEETA*BEETA-(ATAN(ZEETA/(D-X))-THETR)**2
        IF(NR-0.0) 200,200,2
    2   NRMAX=SQRT(NR*LR)
        IF(NTMAX-NRMAX) 15,25,25
   15   NETMX=NTMAX
        NETMN=-NETMX
        GO TO 35
   25   NETMX=NRMAX
        NETMN=-NETMX
C*****************************************************************
C
```

```
C
C       THIS PROGRAM SOLVES THE SCATTER INTEGRAL
C       FOR SCATTER INTEGRAL SOLVING, SIMPSON'N METHOD OF INTEGRATION IS
C
   35   JJ=    20
        RJ=FLOAT(JJ)
        AP=(ZTMAX-ZTMIN)/RJ
        ZTLOW=ZTMIN
        DO 50 I=1,JJ
        Z1=ZP-NETMX*COS(GAMA)
        Z2=ZP+NETMX*COS(GAMA)
        DO 45     LL=1,NOL
        IF(H1(LL)-Z2) 61,45,45
 61      IF(H2(LL)-Z1)  45,45,62
 62     IF(H1(LL)-Z1) 64,67,67
 64     ALLT=Z1
        GO TO 68
 67      ALLT=H1(LL)
 68      IF(H2(LL)-Z2)  36,36,37
 36       UPLT=H2(LL)
         GO TO 29
 37       UPLT=Z2
   29   W=UPLT-ALLT
        AR=(NETMX-NETMN)/RJ
        NEETA=NETMN
        DO 45  KK=1,JJ
        IF(K-1) 16,16,17
 17     YNU=ZETAP*COS(GAMA)+NETMN*SIN(GAMA)
        IF(YLMT-YNU) 45,16,16
 16     CONTINUE
        Z=(ZTLOW*ZP-NEETA*YP)/DEN
C
C       HS IS THE HEIGHT OF TH E SCATTERING LAYER
C
        HS=Z-HPRIM
         DELH=Z-ALLT
        IF(DELH-0.0) 50,6,6
    6  IF(DELH-W) 3,200,200
   3    CONTINUE
        H=(XMAX-XMIN)/RJ
        XI=XMIN
        NUM=JJ/2
        DO 40  M=1,NUM
        FUNC=FUNC+H*(F(XI)+4.*F(XI+H)+F(XI+2.*H))/3.
         PRWAT(J)=PRWAT(J)+1.91*.0001*CN*PT*SKSQ*FUNC*ALAMD**(5./3.)*1000
        IF(PRWAT(J)) 200,200,21
 21     PRDBS(J)=10.*ALOG(PRWAT(J))/ALOG(10.)
   40  XI=XI+2.*H
```

```
   45 NEETA=NEETA+AR
 50    ZTLOW=ZTLOW+AP
       YLMT=ZETAP*COS(GAMA)+NETMN*SIN(GAMA)
  200    CONTINUE
C
C
C
       WRITE(TN,114) THETA,GMADG,PRWAT(J) ,PRDBS(J)
 114   FORMAT(5X,4(E15.8,3X))
       WRITE(TN,129) ALNTH ,THETA
  129  FORMAT(2X,'LENGTH OF COMMON VOLUME=',E15.8,2X,'THETA=',E15.8/)
       IF(YP-20.E 03) 55,56,56
  55   Y=Y+DELY
       GO TO  5
 56    IF(XP-20.E 03) 57,58,58
 57    XP=XP+DELX
       GO TO 9
 58    IF(HT-8.E 03) 59,60,60
 59    HT=HT+3.E 03
       GO TO 8
   60   STOP
       END
// FOR
       FUNCTION F(X)
       REAL NEETA,LT,LR
        INTEGER TN
       COMMON//XP,ZETAP ,NEETA,ZTLOW ,THETA ,FO
C
C
        TN=1
       PI=4.*ATAN(1.)
       D=165.E 03
       THETT=ATAN(ZETAP/(D+XP))
       THETR=ATAN(ZETAP/(D-XP))
C
C
       TB=NEETA*NEETA/((D+X)**2+ZTLOW*ZTLOW    )
       TBB=(ATAN(ZTLOW/(D+X))-THETT)**2
       BETAT=SQRT(TB+TBB)
C
C
       TR=NEETA*NEETA/((D-X)**2+ZTLOW*ZTLOW )
       TRR=(ATAN(ZTLOW/(D-X))-THETR)**2
       BETAR=SQRT(TR+TRR)
C
C
       PAI=PI/180.
C
```

```
      BETDG=BETAT/PAI
   88 BERDG=BETAR/PAI
C
C     THEMAXIMUM VALUE OF THE ANTENNA GAIN HAS BEEN USED AS 42 DBS.
      GTGR=  EXP(-FO*(BETDG*BETDG+BERDG*BERDG)) *10.**(8.4)
      LT=(D+X)**2+ZTLOW**2
      LR=(D-X)**2+ZTLOW**2
C
      THTRD=ATAN(ZTLOW/(D-X))+ATAN(ZTLOW/(D+X))
C
      A=SIN(THTRD/2.)**(11./3.)
C
C
      F=GTGR/(LT*LR*A)
      RETURN
        END
// XEQ MAIN
*CCEND
$ENTRY
C
C     THIE ABOVE PROGRAM WHICH HAS BEEN DEVELOPED FOR IBM 1800 MACHINE
C     CAN VERY CONVENIENTLY CONVERTED TO BE USED ON IBM 7044 BY THE
C     CHANGE OF THE CONTROL CARDS AND THE FORMAT STATEMENTS SUITABLY.
C
C     USE SUITABLE CONTROL CARDS.
C     USE SUITABLE DATA
C
```